Tectonic evolution of the Himalayan syntaxes – the view from Nanga Parbat

ROBERT W.H. BUTLER

School of Geosciences, University of Aberdeen, Kings College, Aberdeen AB24 3UE, United Kingdom.

Orcid: R.W.H.B., 0000-0002-7732-9686
Correspondence: rob.butler@abdn.ac.uk

Abstract: Current tectonic understanding of the Nanga Parbat Haramosh massif (NPHM) is reviewed, developing new models for the structure and deformation of the Indian continental crust, its thermo-rheological evolution and relationship to surface processes. Comparisons are drawn with the Namche Barwa Gyala Peri massif (NBGPM) that cores an equivalent syntaxis at the NE termination of the Himalayan arc. Both massifs show exceptionally rapid active denudation and riverine down-cutting, identified from very young cooling ages measured from various thermochronometers. They also record relicts of high pressure metamorphic conditions that chart early tectonic burial. Initial exhumation was probably exclusively by tectonic processes but the young, and continuing emergence of these massifs reflects combined tectonic and surface processes. The feedback mechanisms implicit in aneurysm models may have been over-emphasised, especially the role of syn-kinematic granites as agents of rheological softening and strain localization. Patterns of distributed ductile deformation exhumed within the NPHM are consistent with models of orogen-wide gravitation flow with the syntaxes forming the lateral edges to the flow beneath the Himalayan arc.

Abrupt changes in the map-trend of orogenic belts and their component sutures, thrusts and folds – so-called syntaxes – are common to many parts of the Tethyan collision system. The purpose here is to review the tectonic evolution of the Himalayan syntaxes (Fig. 1). They include crust that is experiencing

exceptional exhumation rates that provide not only opportunities for relating the rates of tectonic and surface processes but also ideal sites for deducing deformation processes at various scales to understand deformation localization in the crust. They also provide outcrop access to the most northern parts of the Indian continental crust and thus can inform discussions on the deeper structure of the main Himalayan belt. These themes are explored here. However, this review also summarises detailed accounts of the basic geological relationships and the deductions that can be drawn from them, especially for the Nanga Parbat area. An underlying tenet here is that these relationships are fundament for establishing the tectonic evolution and thus for testing and exploring the consequences of models not only those that link denudation to deformation of the continental crust but also strive to explain the evolution of Himalayan orogen as a whole. Without this information it is difficult to assess the uncertainties in the applications of these models.

There are various explanations for the development of non-linear orogenic systems (e.g. Carey 1955; Marshak 1988), as primary arcuate forms or as quasi-linear belts that are subsequently bent, or are folded as they develop. The modern mountain front in the western part of the Himalayan system (Pakistan) contains various types. This front changes trend to form a re-entrant from the western Salt Range, to the Trans-Indus Range (Fig. 1). This pattern can be readily interpreted as a primary structure relating to the extent of propagation of the basal detachment to the thrust system into the foreland, reflecting in turn the subcrop of Cambrian-age halite (Butler et al. 1987). Elsewhere the thrust front along the Kirthar and Sulaiman ranges (Fig. 1) may reflect changes in the geometry of inherited basement rift structures in controlling collision-related contractional tectonics (e.g. Coward 1994). Tectonic rotations and local transverse folding of pre-existing structures may result from interacting, doubly-vergent thrust systems within an overall zone of parallel convergence (e.g. in the Eastern Salt Range; Butler et al. 1987). Thus the mountain front has evolved in plan view.

While some syntaxes develop at or near the active mountain front, within the main Himalayan chain there are much larger structures. It is these that form the principal focus of this review. The Himalayan arc (Fig. 1) extends for 2500

km but terminates abruptly at each end at two major antiforms around which structures loop in map-pattern. These are the Himalayan syntaxes – cored by the Nanga Parbat-Haramosh massif (in the NW: NPHM) and the Namche Barwa – Gyala Peri massif (in the NE: NBGPM). They characterized by exceptionally fast rates of erosion and bed-rock exhumation, and consequently provide outcrops of levels of collided Indian continental crust that otherwise would lie deeply buried beneath their orogenic cover. The two districts have significantly different histories of geological research (Fig. 2) - reflecting their contrasting logistical challenges.

The NPHM (Fig. 3) has been accessible for almost a century, through a track network that serviced the frontier town of Gilgit. The terrain is exceptionally rugged, with some of the greatest relief on Earth, rising to the peaks of Nanga Parbat (8125m) and Haramosh (7397m; Figs. 3 and 4). The mountains are transected by deep gorges, including that of the Indus (Fig. 4c, d). Thus early geological research was chiefly allied to mountaineering expeditions, aimed at creating reconnaissance geological maps (e.g. Desio 1964). Construction of the Karakoram Highway (KKH; Fig. 4c) through the 1960s and 70s allowed geologists, principally from Peshawar University, to create regional maps (e.g. Tahirkheli and Jan 1978). The KKH opened to international visitors in 1979, which together with its offshoots further up the Indus gorge to Skardu (Fig. 4d) and up the Astor valley (Fig. 2), kick-started more detailed investigations of the NPHM. These western areas of the Greater Himalaya are relatively arid (e.g. Finlayson et al. 2002) and so provide exceptional outcrop. It has also benefitted being under a single administrative control (Pakistan). The SE portion of the NPHM, where its geological linkages into the main Himalayan arc can be established, lies on the original access (pre- Karakoram Highway) to Gilgit from the south. It is restricted due to proximity to the disputed Pakistan-Indian border. However, wider security to the whole region for international visitors has been difficult since 2001, especially so after the murder by a Taliban sect of eleven members of mountaineering expeditions to the Daimir face of Nanga Parbat in June 2013.

In contrast, the NBGPM lies within the Tibet Autonomous Region with access very strictly controlled by the Chinese authorities. Research activity has

100 accelerated over the past 18 years (Fig. 2), especially with the increased
101 involvement of Chinese earth scientists. Unlike the western syntaxis, there is no
102 equivalent to the KKH-Skardu road providing simple access for transects
103 through the NBGPM – even if authority controls were relaxed. Both syntaxes are
104 still significantly under-represented on geological maps - their internal structure
105 and basement stratigraphy remains incompletely established. Yet the NPHM
106 especially has been a testing ground for novel methods in quantifying tectono-
107 geomorphological processes and rates, as reviewed below, but rarely have these
108 methods been applied more broadly through their study areas. Consequently
109 this review, as others before (e.g. Khan et al. 2000), should not be read as a
110 definitive record but rather as a summary of a transient state of the art. The
111 narrative here focuses primarily on NPHM but then draws comparisons with
112 NBGPM.
113 The geology and history of research through the 20th century at Nanga
114 Parbat, and more generally in the NW Himalayas, have been extensively
115 reviewed by Khan et al. (2000). Research, especially relating to new fieldwork,
116 has fallen away since then – with subsequent papers focussing on the young
117 tectonic history of the NPHM – essentially building up on and examining the
118 consequences of Zeitler et al.'s (2001) tectonic aneurysm model. This concept is
119 developed from the notion that crustal shortening is balanced against the
120 thickness of the crust and that syn-kinematic erosion permits crustal shortening
121 to progress (e.g. Beaumont et al. 1992; Willett 1999). However, the aneurysm
122 model incorporates the thermal consequences of rapid exhumation that drives a
123 positive feedback between deformation and erosion. Exhumation elevates the
124 transition from depth-dependent friction sliding (faulting) which effectively
125 reduces not only the maximum but also the integrated strength of the deforming
126 crust. Zeitler et al.'s (2001) model proposes that, if exhumation is rapid enough
127 to drive decompression melting, the syn-kinematic crustal melts weaken the
128 crust, focusing deformation further. This in turn accelerates deformation,
129 generating faster uplift rates with concomitant accelerating erosion and
130 exhumation. Thus syn-tectonic crustal melting is generally assumed to be the
131 critical influence on the dynamics – a deduction common not only to the syntaxes
132 but also to other parts of the Himalayan collision system. Both syntaxes have

become test-beds for developing analytical strategies for understanding the interactions between Earth surface processes and the thermo-tectonic evolution of the continental crust in collision belts.

The pre-exhumation tectono-metamorphic evolution of the Nanga Parbat - Haramosh Massif

Although the principal modern interest in the NPHM lies in its Plio-Quaternary history, understanding the aneurysm model and its limitations demands understanding the precursor geology of the massif. As Whittington and Treloar (2002) point out, the distribution and concentration of key reactants - muscovite and biotite – will control the sites of decompression melting and leucogranite genesis. The preceding burial and heating histories of the massif are also important. These earlier parts of the geological history also have a bearing on the development of the India-Asia collision in the NW Himalayas. There follow discussions on the basement geology and pre-uplift structural history of the massif that are concluded by examining implications for the early collision history. These then provide information on the conditions that pertained at the start of the late Neogene exhumation history, as discussed later.

Basement structure

That the heart of the NPHM contains abundant migmatitic gneisses (Fig. 5) has been established since the early syntheses of Wadia (1919) who ascribed them to the Archaean, in common with assumptions made for many high-grade metamorphic terranes at the time. Misch (1949) demonstrated that the migmatites, with cordierite-K-feldspar-sillimanite assemblages, pass laterally into lower-grade metasediments on the flanks of the massif (Fig. 3). Since the initial studies of gneiss types by Madin et al. (1989) in the 1980s, there have been sporadic attempts to unravel basement geology at Nanga Parbat. Zeitler et al. (1989) report ion microprobe U-Pb profiles in zircon with core ages of c 1850Ma and rims at 2.3-11Ma. In the absence of field relationships, relating geochemical data from accessory phases to the structure, and therefore the

166 tectonic evolution of the massif has been ambiguous (but see Crowley et al. 2009,
167 discussed below). The challenge has been to establish how much of the basement
168 structure relates to Himalayan tectonics and how much was inherited from the
169 earlier crustal history of the Indian continent. The discovery of suites of mafic
170 intrusions that cross-cut gneissic fabrics throughout the massif (Butler and Prior
171 1988a; Wheeler et al. 1995) indicates that the rocks experienced pre-Himalayan
172 metamorphism (see discussion in Whittington et al. 2000). Treloar et al. (2000)
173 conclude that the migmatitic fabrics in the heart of the massif are Precambrian in
174 age (but see Crowley et al. 2009, discussed below).
175 Sr and Nd isotopic data show that the NPHM is assembled from pre-
176 Himalayan metamorphic units (Argles et al. 2003) that correspond to the
177 distinctive basement terrains (Lesser Himalayan, High Himalayan) of the main
178 Himalayan belt. However, unlike the main Himalayas, at NPHM these different
179 basement units do not lie in distinct Himalayan thrust sheets. No such structure
180 can be mapped and indeed it is difficult, using field relationships alone, to
181 establish which unit is which in the core of the massif. Around the flanks, non-
182 migmatitic metasediments, chiefly biotite schists and psammites are cross-cut by
183 biotite granites, commonly with large feldspars. These field relationships match
184 those in the Hazara hills of the outer parts of the Pakistan Himalayas, where, late
185 Proterozoic metasediments are intruded by 500-600Ma peraluminous granites
186 (e.g. Baig et al. 1988). These granites (both in Hazara and NPHM) deform into
187 augen-gneiss that can be mistaken for Proterozoic migmatitic gneiss. The massif
188 may be one of the few regions that could resolve the pre-collisional structural
189 relationships between various basement units on the northern margin of the
190 Indian continent – but as yet these are unresolved. The margins of the NPHM are
191 marked by a discontinuous veneer of metasediments without biotite granite
192 intrusions and with distinctive marbles. These are speculatively correlated with
193 the “Tethyan series” of cover sediments (Butler and Prior 1988a). That these
194 units are not significantly interleaved with the basement units described above
195 suggests that the NPHM contains little basement-cover imbrication of Himalayan
196 age and therefore that it behaved as a coherent tectonic unit during the collision.
197
198 <u>Relationship with Kohistan-Ladakh arc</u>

At the present outcrop level, the boundary between the NPHM and the surrounding Kohistan-Ladakh arc terrain is composite – in part defined by cataclastic faults signifying young deformation together with significantly earlier ductile structures. This early ductile structure was correlated with the Main Mantle Thrust (MMT), the southern suture of the Kohistan-Ladakh arc with the Indian continental crust defined 150 km WSW of Nanga Parbat (e.g. Tahirkheli and Jan 1979). It has been recognized in the Indus gorge (Butler and Prior 1988a), along the northern plunge termination of the massif (Fig. 6a; Butler et al. 1992; Pognante et al. 1993) and along its eastern margin (Fig. 6b; Argles 2000). It is an amphibolite facies shear zone, many hundreds of metres thick (Fig. 6a). In its hangingwall in the western Indus gorge (Fig. 6c), the shear zone deforms suites of granite sheets (the Confluence and Parri suites of George et al. 1993). Away from the shear zone these form cross-cutting networks but they are sheared, boudinaged and tightly folded in the shear zone (Fig. 6d,e). Ubiquitous top-to SSE kinematics are displayed by these deformed Kohistan rocks (Fig. 63) The same kinematics are displayed by shear bands and asymmetric boudinage in the deformed metasediments of the NPHM in the footwall (Fig. 6f). Argles (2000) notes the equivalent kinematics, represented as right-lateral shear, along the steep eastern margin of NPHM in the upper Astor valley.

The Confluence and Parri granite sheets were derived from a juvenile arc source, without contamination from Indian continent rocks. They comprise two distinct suites, one dated at 50-32 Ma and a younger Rb-enriched set dated as early Miocene (c. 26 Ma). That these intrusions are deformed into the ductile shear zone dates this structure was active until at least 26 Ma. The shear zone cannot be the original suture between the Indian continent and the Kohistan-Ladakh arc and is therefore not the MMT as defined elsewhere to the west (c.f. Butler and Prior 1988a). Butler et al. (1992) termed the structure the *Phuparash Shear Zone* – a name used here to designate the amphibolite-facies tectonic contact between the Kohistan arc terrain and rocks of the Indian continent now preserved in the NPHM but which predates the late exhumation of the massif. The geochemistry of the Confluence and Parri granites places a limit on the northward extent of the NW Indian continent beneath the leading edge of the

232 amalgamated Asian continent prior to Miocene times. This is discussed further
233 below.
234
235 Tectonic burial of the Indian continental crust
236
237 The NPHM is best known for its HT/LP metamorphism reflected in extensive
238 development of migmatites. The preserved PT- conditions of these rocks are
239 presented in two transects through the massif (Fig. 7a,b) and these are discussed
240 later. However, the interleaved metasedimentary and meta-igneous rocks (the
241 'Layered Unit" of Butler et al. 1992) of the northern part of NPHM locally
242 preserve eclogitic assemblages within metabasic rocks (Pognante et al. 1993).
243 Termed the "Stak eclogites", they record peak conditions of c 2.5 GPa, c 750C
244 (Lanari et al. 2013; Fig. 7c). They are extensively overprinted by amphibolite
245 facies mineral assemblages (c 0.7 GPa, 650C) that have all but obliterated the
246 eclogitic assemblages. These HP conditions were likely far more widespread
247 through the massif. Kouketsu et al. (2016) report U-Pb zircon ages that
248 tentatively date the thermal overprint at 36-28 Ma, broadly in the range of ages
249 for the thermal maximum in NPHM of Foster et al. (2002). They contrast these
250 results with those obtained from the coesite-bearing eclogites of the Kaghan
251 valley (c 100 km SW of the Stak eclogites), where peak conditions of c 3 GPa and
252 700C were achieved at c 45-47 Ma , and the rocks exhumed to the mid crust by c
253 44 Ma. Thus rather than be rapidly exhumed, the NPHM resided longer at lower
254 crustal levels than the Kaghan eclogites. The thermal consequences of this
255 extended residence may explain the sparse preservation of HP assemblages in
256 the massif.
257
258 Early Himalayan tectonic history of NPHM
259
260 The igneous history of Kohistan and the tectono-metamorphic history of the
261 NPHM raise issues for the evolution of the NW Himalayas. These can be
262 represented on scaled cross-sections (Fig. 8). The Stak eclogites – preserved in
263 the outermost metasediments of the NPHM - suggests that the Indian crust upon
264 which these rocks lay was subducted beneath the frontal (southern) part of the

Kohistan arc terrain. A similar setting is presumed for the genesis of the Kaghan eclogites. The Stak eclogites achieved peak pressures before c 36 Ma – potentially as early as 45-47 Ma if burial was synchronous with that of the Kaghan eclogites. Uplift and partial unloading of the Stak eclogites to c 07.GPa by 36-28 Ma requires removal of some of the overburden. This is broadly contemporaneous with granite genesis in the now-overlying Kohistan arc terrain. But granite genesis and eclogite exhumation initially must have been spatially separated – the Kohistan granites show no contamination by Indian continental crust. Their juxtaposition, and much of the displacement on the Phuparash shear zone, must be rather late. Note that the shear zone omits the lower part of the Kohistan arc terrain and therefore contributes to exhumation of the Stak eclogites by tectonic processes.

Thus before the younger tectonic episodes that saw it exhumed to the surface, the NPHM resided in the lower part of a duplicated crustal stack, capped by the residual Kohistan arc terrain. The tectonic contact between the Indian continental crust of the massif and arc terrain above was the Phuparash Shear Zone. It was from this position, with its cover series buried at c 30 km depth, that the NPHM was exhumed during late Neogene times. The cross-section gives a direct measure of the burial state of the Indian continental crust, and by inference, the rocks preserved at outcrop in the NPHM. The shallow parts of the Indian crust (the "layered unit" of Butler et al. (1992)) lay at 0.7 GPa, with the underlying crust at correspondingly higher pressures. Presumably temperatures in this buried Indian crust were c 650 – 750 C, gradually warming into the onset of exhumation tectonics.

Tectonics, metamorphism and melting: the exhumation of the Nanga Parbat – Haramosh Massif

Various interpretations for the current structure of the NPHM have been proposed (Fig. 9). Note that all these recognize the broadly antiformal structure to the massif depicted by the trace of the tectonic contact between the massif and the structurally-overlying Kohistan Arc Terrain. This contact is generally termed the Main Mantle Thrust and is labelled as such on Fig. 9 in accordance with the

298 original authors. However, as discussed above, this structure is better given an
299 alternative name (the Phuparaash Shear Zone) as it is a distinctly younger shear
300 zone to the MMT in its type area some 150km SW of Nanga Parbat.
301 Based on the Indus gorge transect, Coward (1985) defined the broad
302 antiformal structure of the massif, an interpretation followed by more detailed
303 structural studies by Wheeler et al. (1995; Fig. 9a). Upright folding was also
304 proposed for the internal structure of the massif along the Astor valley transect
305 by Argles and Edwards (2002). Burg and Podladchikov (2000) developed
306 numerical models to investigate crustal scale buckling and crustal strength in
307 syntaxes. These models predict uplift of the Moho beneath the NPHM.
308 Based on structural studies along the western margin of the massif, Butler
309 and Prior (1988b) argued that the massif was carried on a NW-directed ductile-
310 to brittle thrust zone (the Liachar Thrust; Fig. 9b). Their NW-SE oriented section
311 (Butler et al. 1988) through the Chongra district predicted uplift of the massif's
312 thermal structure together with hydrothermal activity focused on the Liachar
313 thrust. It is this structure that overprints the earlier tectonic contact with the
314 Kohistan Arc Terrain. In contrast, the eastern margin of the massif was predicted
315 to simply be marked by the early ductile shear zone (MMT/Phuparash Shear
316 Zone) between the Kohistan Arc terrain and the Indian continental crust.
317 Regional geological studies around the entire Nanga Parbat area led
318 Schneider et al. (1999; Fig. 9c) to propose that the massif was uplifted on two
319 opposed thrust-sense shear zones – the NW-directed Daimir shear (essentially
320 the lateral continuation of the Liachar structure of Butler and Prior 1988b) and
321 the SE-directed Rupal shear zone. This defines a "pop-up" structure, an
322 interpretation that lies at the heart of Zeitler et al.'s (2001) aneurysm model for
323 positive feedback in crustal deformation. This model requires the Rupal and
324 Diamir Shear Zones to be broadly contemporaneous – and certainly active during
325 leucogranite genesis and exhumation. Syn-kinematic granite melt emplaced into
326 both shear zones is inferred to reduce their strength thereby focusing further
327 deformation.
328 Butler et al. (2002) argued that the role of localized shear zones in
329 accommodating uplift of the massif had been exaggerated and that deformation
330 was largely achieved by vertical stretching, distributed through the heart of the

massif. This model is invoked by Crowley et al. (2009) to explain the localized uplift and exhumation of the heart of the massif.

Thus although interpretations show the massif to have a broadly antiformal structure, they vary in consideration of which structures within the massif relate to its exhumation and which were developed in earlier Himalayan deformation (or be part of pre-collisional Indian continental geology). These issues, and the merits of the various models, are discussed below after reviewing structural observations and other geological data.

Geophysical constraints

The deep structure of the NPHM and adjacent regions has been determined geophysically. Gravity anomalies suggest a relatively smooth Moho across the syntaxis, at a depth of 65-70 km (Tiwari et al. 2015). This is broadly consistent with the crustal thickness determined from teleseismic receiver functions to the east of the syntaxis (Rai et al. 2006). There is no indication of the upwarped Moho predicted by the numerical models of crustal buckling developed by Burg and Podladchikov (2000). This model is therefore inappropriate to explain the crustal structure.

Magnetotelluric profiling by Park and Mackie (2000) show the crust beneath Nanga Parbat to have high resistivity from which they conclude that it is dry and restitic, without any discernable in-situ melt. In contrast the uppermost few km are more conductive – interpreted as revealing a weakly connected, fracture-hosted network if aqueous fluid. This is consistent with the prediction of Butler et al. (1988; Fig. 9b). Fluid inclusion studies of synkinematic veins by Craw et al. (1994) subsequently established the hydrothermal system, driven by by meteoric water from the mountain peaks in the heart of the massif. They proposed that the system penetrated to c 5 km. This depth lies slightly above the zone of microseismicity mapped by Meltzer et al. (2001), This indicates that the "brittle-ductile" transition along the Liachar thrust zone lies significantly shallower than that schematically illustrated by Butler et al. (1988; Fig. 9b).

Late Himalayan metamorphism and granites

The NPHM contains some of the World's youngest collision-related granites (Zeitler et al. 1993), as reviewed extensively by Whittington and co-workers (Whittington et al. 1999; Whittington and Treloar 2002). Collectively these leucogranites have formed the cornerstones to Zeitler et al's (2001) aneurysm model and its derivatives (e.g. Koons et al. 2002) and are generally assumed to have substantially weakened the crust. The leucogranites have various forms. Almost all are feldspar-quartz rocks with white mica and tourmaline and they form different types of intrusion (Fig. 10). There are few km-sized intrusions with cm-mm grain-sizes (Fig. 10a, shown on Fig. 3). However, the massif is riddled with m-10sm width leucogranite sheets (e.g. Fig. 10b), most of which are coarsely pegmatitic. One of these, near Tato village, yielded a crystallization age of 0.7 Ma (Crowley et al. 2009). Where studied (Butler et al. 1992; Whittington et al. 1999), the plutons yield high Rb-Sr ratios and very high ^{87}Sr-^{86}Sr ratios that collectively imply vapour-absent, muscovite melting of a metapelite source. Similar values are obtained for the leucogranite pegmatites. Whittington and Treloar (2002) propose the reaction:

22 Muscovite + 7 Plagioclase + 8 Quartz = 25 melt + 3 K-feldspar + 5 Sillimanite + 2 Biotite

Melt volumes are controlled by the proportion of muscovite in the source, with the mass of leucogranite generated by this reaction only slightly more than that of the muscovite consumed by the reaction.

Relating leucogranites to migmatitic source-areas within the massif is difficult: the poly-metamorphic history of the Indian crust renders establishing the pattern of Himalayan metamorphism within the NPHM especially challenging. Poage et al. (2000) compile a range of P-T estimates, chiefly from metapelites, that confirm the general trend noted by early workers, of high peak temperatures in the heart of the massif passing out to lower temperature rocks on the margins. In contrast peak pressures are lower in the heart, increasing to the margins (Fig. 7). The antiformal structure of the NPHM means that the present heart of the massif was more deeply buried than its margins prior to exhumation. Therefore the preserved metamorphic conditions were not

396 achieved synchronously: Poage et al. (2000) suggest that the heart of the massif
397 has experienced younger HT/LP overprinting.
398 Butler et al. (1997) point out that the migmatites currently at outcrop in
399 the NPHM are unlikely to be the main source for the leucogranites – because the
400 main migmatitic fabrics are cross-cut by pre-Himalayan mafic dykes. Certainly
401 the Tato pluton has Sr-isotopic values outside those of adjacent metasediments
402 (Whittington et al. 1999). Consequently Whittington et al. (1999) argue that
403 their source remains buried and that the melt migrated several km up through
404 the crust to be emplaced in the plutons and arrays of leucogranite pegmatite.
405 that riddle the massif.
406 However, the Tato-upper Raikhot area (Fig. 3) show secondary
407 migmatitic textures (Fig. 10d). Crowley et al. (2009) propose the vapour-absent
408 biotite melting reaction:
409 Biotite+Sillimanite+Plagioclase+Quartz = Cordierite+Garnet+K-feldspar+melt
410 These melts only migrate very short distances, if at all, as the
411 crystallization of cordierite takes water and thus increases the viscosity of the
412 residual melt. These *in situ* migmatites yield peak temperatures of 730 ˚C (±30
413 ˚C) at 350 MPa (±30 MPa) while the formation of garnet-cordierite melts
414 suggests conditions of 720 ˚C (±20 ˚C) at 500 MPa (±30 MPa). Monzaite
415 crystallization ages for these rocks yield ages of 1660 ± 15 ka, interpreted as the
416 date of these peak conditions.
417 The Nanga Parbat area therefore charts two distinct melting processes,
418 which operated synchronously but at different crustal levels (Whittington and
419 Treloar 2002). Both involve decompression and therefore relate to the
420 exhumation of the NPHM. Thus melting relates to denudation.
421
422 <u>Geomorphology and thermochronology</u>
423
424 Key to the denudation of the Nanga Parbat massif and its surroundings is the
425 Indus river and its tributaries. The erosive power of these systems retains the
426 rivers at remarkably low elevations. At Raikhot (Fig. 3) the Indus is just 1100m
427 above sea level, with the summit of Nanga Parbat (8125m) just 21 km away (Fig.
428 4a). The combined influence of glaciation and catastrophic rock slope failures

429 governed by the relief and maximum elevations deliver sediment to the river
430 system (e.g. Hewitt 2009). Rivers then transport the load away from the
431 mountains, freeing the lower slopes for the receipt of the erosional products of
432 further glaciation and slope failure.
433 The NPHM has been a test-bed for applying thermochronological and
434 geomorphological methods in the understanding of active tectonics in mountain
435 belts. These include the early application of multi-mineral fission track studies to
436 quantify patterns of low-temperature cooling (Zeitler et al. 1982; Zeitler 1985)
437 and the use of cosmogenic (^{10}Be, ^{26}Al) exposure age dating to chart bedrock
438 erosion (Leland et al. 1997). These studies have focused on the Indus gorge,
439 which provides a natural transect through the massif. Leland et al. (1997) argue
440 that incision rates on the Indus have increased from c 4-6 m/ka at 27-65ka to 10-
441 14 m/ka in the past 7ka, where it passes through the NPHM, significantly faster
442 than to the east. This zone of enhanced down-cutting matches the young fission
443 track ages obtained from apatite and zircon (Zeitler et al. 1982; Fig. 11) that
444 imply cooling rates of up to 120 °C/Myr for the Indus gorge. The fission track
445 data are asymmetric, with fastest cooling at the western end of the Indus gorge,
446 just upstream from the confluence with the Gilgit River.
447 Ar-Ar isotopic data from amphiboles and white mica have been obtained
448 widely around the massif (Treloar et al. 2000; Schneider et al. 2001) – again
449 largely aimed at resolving the pattern of cooling from which the denudation
450 history might be deduced. Similarly, perched terraces and dissected strath levels
451 have been mapped through the Nanga Parbat area and tentatively correlated
452 with the glacial history of the NW Himalayas to estimate valley down-cutting
453 rates (e.g. Schroder and Bishop 2000). All of these methods have problems. It is
454 now realized that geomorphological rate estimates depend upon the observation
455 time-scale, ignorance of which introduces significant bias (DiBiase 2014). Argon
456 isotopes can be unreliable chronometers where radiogenic argon can be
457 incorporated into minerals, to be expected in metamorphic terrains (e.g. Warren
458 et al. 2012). And simply relating palaeo-thermal data to unroofing depends upon
459 palaeo-geotherm, which in active, rapidly denuding locations may be challenging
460 to resolve (e.g. Whittington 1996). Notwithstanding these limitations, these
461 quantitative methods yield results that are broadly consistent with the time-

averaged exhumation rates deduced from regional cross-sections and as deduced by qualitative analysis of the original fission track data from the Indus gorge (Zeitler et al. 1982; Fig. 11).

Young/active structures on the western margin of the massif

Active deformation at NPHM is indicated by microseismicity, apparently restricted to the top 5km of the crust (Meltzer et al. 2001). Recent work has identified right-lateral focal mechanism on the western margin, together with weak normal faulting in the interior of the massif (Mukhopadhyay et al. 2011). GPS-derived velocity fields do not resolve any net convergence across the massif as a whole (Jouanne et al. 2014), albeit based on a very short observation window of 4-5 years. There is a residual weak E-W convergence of the heart of the massif relative to Kohistan of 2-7mm/a, apparently accommodated on the western margin of the massif. There is no detectable convergence across the eastern margin. Jouanne et al. (2014) argue that the active seismicity and geodetic strain represent dominantly vertical flow of the NPHM relative to its surroundings with weak E-W contraction matched by weak extension in the heart of the massif.

Relating active deformation structures and their structural kinematics to vertical motions within the NPHM is obviously fundamental to understanding tectonic processes. Yet there is significant confusion in the literature concerning the nomenclature of faults and shear zones associated with the NPHM, especially along the western margin (reviewed by Butler 2000). Lawrence and Ghauri (1983) coined the term “Raikhot Fault” and this has been adopted for the entire western bounding structure of the NPHM by Madin et al. (1989) and some others since (e.g. Jouanne et al. 2014). In the author’s view this obscures tectonic understanding as it conflates different structures of different ages that coincide only locally but otherwise diverge around the massif. Furthermore, the original structure interpreted by Lawrence and Ghauri (1983) is part of a major landslip (Butler and Prior 1988b; Butler et al. 1988; Hewitt 2009) and has no continuity into the bedrock. Consequently, the more precise terminology of Butler (2000) is followed here.

The most prominent active structure is the *Liachar Thrust* (Butler and Prior 1988b) that carries highly sheared gneisses with leucogranite sheets onto unconsolidated sands and gravels of the Indus valley (Fig. 12a). It is probable that seismicity on this structure at depth triggered the array of catastrophic landslips, including the 1840-41 events that dammed the Indus (Butler et al. 1988; Hewitt 2009; Fig. 4c). There are arrays of related faults developed in both the footwall and hangingwall to the Liachar Thrust, with distinct orientations and character that may relate to the orientation of host rock fabrics (Butler et al. 2008).

Along with the Liachar Thrust, there are significant north-south trended cataclastic structures, many of which show strike-slip kinematics (Butler et al. 1989). These may be traced north to the Indus gorge (e.g. Madin et al. 1989) to link into the *Shahbatot fault* system (Fig. 12b; Butler et al. 1989). Collectively the cataclastic system accommodates transpression, with NW-SE contraction together with right lateral strike-slip.

Brittle deformation is strongly focused along the western margin of the massif, and this is reflected in the original thermo-chronological studies that show asymmetric cooling (Zeitler et al. 1982). However, the thermochronology and down-cutting estimates are from the Indus gorge – where the neotectonic structure is RL strike-slip, not reverse – as assumed by Leland et al. (1998). The strike-slip regime may however be rather young – and overprint earlier contractional structures – which could explain why the nick-point on the Indus is not situated at the active fault strand but is 30 km upstream (Leland et al. 1998). The offset could reflect upstream migration following a local switch in tectonic kinematics.

A new cross-section

A new cross-section through the NPHM is presented (Fig. 13) which shows active surface-breaking faulting to be restricted to the western margin of the massif. This is the Liachar Thrust. However, unlike earlier interpretations (Butler and Prior 1988b; Fig. 9b) the thrust zone is only developed near-surface. Deeper

527 parts of the massif, and the outcropping heart, contain near-vertical stretching
528 strains (Butler et al. 2002).
529 The central challenge in elucidating the deformation structures that,
530 along with denudation, have accommodated exhumation of the NPHM over the
531 past few million years lies in discriminating these from earlier deformation. As
532 Wheeler et al. (1993) point out, it is a standard problem in multi-deformed
533 basement terrains. However, just as they use basic sheets to identify pre-
534 Himalayan structures, syn-exhumation leucogranites may be used to identify
535 exhumation-related structures (Fig. 10).
536 Deformed leucogranite pegmatites are found throughout the Liachar
537 shear zone indicating that it is a young structure (Fig. 10e-i; Butler and Prior
538 1988b). Likewise the heart of the massif around Tato village contains
539 leucogranite seams that relate directly to boudin necks that indicate sub-vertical
540 stretching occurred during exhumation (Fig. 10c; Butler et al. 2002). However,
541 there are no such descriptions from the Rupal Shear Zone – although much of the
542 critical ground lies on the inaccessible southern cliffs of Nanga Parbat. No
543 leucogranites are described by Butler et al. (1992) for the Rama outcrops
544 between Astor and Chongra peak. Therefore it is possible that the Rupal Shear
545 Zone is not part of the exhumation of the massif. Furthermore, the Rupal Shear
546 Zone does not cut the ductile shear zone on the eastern margin of the NPHM (the
547 continuation of the Phuparash Shear Zone). A new interpretation is proposed
548 here (Fig. 13), that the Rupal Shear Zone is an earlier Himalayan structure,
549 unrelated to the recent exhumation of NPHM. In this model, it branches onto the
550 Phuparash Shear Zone north of Astor village. Argles (2000) points out that this
551 sector of the massif's eastern margin has complex lateral variation so that rock
552 units are difficult to correlate along strike. This would be expected if this area
553 contains early thrust-sense shear zones that repeat stratigraphy. The general
554 northward plunge on the massif allows inferred footwall rocks to crop out
555 further south – marking a transition southwards into decreasing metamorphic
556 grade. These metasedimentary cover may exist at depth beneath the Rupal Shear
557 Zone, continuing beneath the summit of Nanga Parbat and thus may provide a
558 buried source for leucogranites.
559

560 Leucogranites and deformation
561
562 Beyond arguing that melt weakens the shear zones into which it has been
563 emplaced, the aneurysm model, (Zeitler et al. 2001; Koons et al. 2002) does not
564 explain the exhumation of hot rocks act to create or localize deformation onto
565 specific structures. Their schematic illustration shows the structure of the NPHM
566 as a "pop-up" bounded by two thrust-sense shear zones. Yet the chief site of
567 exhumation and main area of anatexis is found within the massif, not simply
568 within the shear zones. Widely distributed anatexis and thermal weakening
569 might rather be expected to generate broad zones of deformation. This
570 expectation is consistent with the kinematic model for crustal deformation at
571 NPHM of Butler et al. (2002) who show general syn-magmatic vertical stretching.
572 The localized shearing that evolves into cataclastic faulting along the western
573 margin of NPHM is then simply a consequence of near-surface cooling.
574 The role of exhumation-related anatexis as a weakening mechanism is
575 developed further by Crowley et al. (2009). They argue that "vertical channel-
576 flow", essentially the pure shear thickening model of Butler et al. (2002), was
577 promoted by the vapour-absent breakdown first of muscovite and subsequently
578 of biotite. They suggest that it was this additional reaction that decreased the
579 effective viscosity of the crust beneath Nanga Parbat leading to in increase in
580 strain rate that in turn drove faster uplift.
581 But is the generation of granitic melt itself sufficient to weaken the rocks
582 within which it resides sufficiently to influence significantly the deformation?
583 The aneurysm model is underpinned by the tacit assumption that the processes
584 of anatexis and granite generation are weakening mechanisms for crustal
585 deformation – a notion dating back at least to Hollister and Crawford (1986).
586 The leucogranite pegmatites of the Liachar shear zone are synkinematic.
587 They cross-cut deformation fabrics but have deformed shapes consistent with
588 top-to NW shearing (Fig. 10f, g, i). In many cases boudin necks show
589 concentrations of quartz and other phases (e.g. Fig. 10h) indicative of
590 structurally-controlled fractional crystallization. In these cases the composite
591 pegmatite body must have deformed during its crystallization. Less-deformed
592 parts of structures, including boudin bodies, are generally characterized by

preserving igneous crystallization textures with the only deformation structures represented by grain fracturing. Similarly, folded pegmatite bodies (Fig. 10 i) contain primary crystallization textures (Fig. 10j), commonly aligned in a many akin on syntaxial crystal growth in hydrothermal veins. Most of the leucogranites within the NPHM simply cross-cut deformation fabrics. In the Liachar shear zone they show predominantly strong inclusion behavior (e.g. Passchier et al., 2005) – indicating that the presence of granite is a strengthening phenomenon. These observations are consistent with the notion that fully crystallized granites strengthen the continental crust (e.g. Neves et al., 1996; Brown, 2013).

For deformation to be melt-enhanced, crystallization rates for melts must be sufficiently slow to be able to accumulate significant tectonic strain and these melts must remain within the deforming rock volume. Observations in the Liachar Shear Zone (Fig. 10) indicate that the pegmatites deformed before full crystallization yet field relationships indicate that at all stages of deformation, the bodies behaved more competently than their surroundings. The implication is that crystallization initiated very rapidly upon final emplacement of the leucogranite melt and outpaced deformation. For these emplaced melts to be effective at weakening the Liachar Shear Zone they would need to have lower strength for time periods sufficient to accumulate significant strain. And this does not appear to have happened.

In contrast, very low melt concentrations that remain *in situ* in the migmatites of the heart of the massif, appear to focus local deformation (Fig. 10c). As Brown and Rushmer (1997) note, melt on grain boundary films can greatly reduce bulk viscosity and thus enhance deformation. However, larger melt fractions are effectively drained from migmatites in veins (e.g. Brown 2013). Thus for melting to enhance the host ductility it must remain *in situ*. And this may explain enhanced vertical stretching, rather than shearing on localized zones, being the primary deformation mechanism within the massif.

Thermo-rheological model.

Strength-depth curves for continental crust generally resolve two distinct domains: near-surface, depth-dependent deformation controlled by pressure-

626 sensitive friction slip (or cataclasis with grain-boundary sliding); and deeper,
627 temperature sensitive creep (crystalline plasticity). The greatest strength in the
628 crust is located at the cross-over between these two domains – the "brittle-
629 ductile transition". As Koons et al. (2002) note while quantifying the aneurysm
630 model of Zeitler et al. (2001), raised isotherms effectively erode the frictional slip
631 domain, thus reducing bulk strength of the crust beneath the Himalayan
632 syntaxes. The thermal structure within the NPHM can be estimated using the PT
633 estimates from Crowley et al. (2009; Fig. 14), with near isothermal
634 decompression followed by very rapid cooling in the final few km of exhumation.
635 The resultant thermal structure may be used to infer strength-depth
636 relationships, using the approach of Handy (1999; inset, Fig. 14). Strain rates of c
637 10^{-12} (strains of 1-3 accumulated over c 1 Myr) are applied to a polymineralic,
638 quartzo-feldspathic rock. This reveals the rather low strength of the upper crust
639 (c 20km – 7 km), rapidly increasing at shallower depths. Using a typical friction
640 coefficient (μ= 0.8) yields at "brittle-ductile transition" at c 5km depth. Note that
641 changing this coefficient to very low values (typical of fault lubricated by
642 serpentinite, halite or swelling clays, none of which are appropriate to the
643 NPHM) will only reduce the "brittle-ductile transition" to c 6 km.
644 The onset of cataclastic deformation at relatively high temperatures,
645 illustrated on the thermo-rheological plot (Fig. 14) was inferred by Butler and
646 Prior (1988b; Butler et al. 1988) and recognized as being unusual. Classical
647 models of brittle-ductile shear zones (e.g. Sibson 1983) depict the transition to
648 occur within the broad greenschist facies, at temperatures around 300 °C – 350
649 °C. The nucleation of earthquakes on these systems happens within a zone
650 controlled by quartz ductility and phyllosilicate-influenced deformation. For the
651 Liachar thrust, and presumably other cataclastic fault zones around the massif,
652 the structure of the seismogenic zone may be significantly different from those
653 inferred elsewhere. Regrettably the only microseismicity monitoring
654 experiments conducted at Nanga Parbat to date (Meltzer et al. 2001) were of
655 insufficient duration to explore this inference.
656
657 **Comparisons with Namche Barwa**
658

As research activity in the Nanga Parbat district has waned, so interest in the eastern syntaxis has increased. It too is dominated by two distinct mountain groups – Namche Barwa (7782m) and Gyala Peri (7294m) – and they are also separated by a deep river gorge, carrying the Yalung-Tsangpo river (Fig. 15). The NBGPM forms a structural half-window framed by the rocks of the Lhasa Block. Much of the original research is reviewed by Bracciali et al. (2016; compare with Zeitler et al. 2014). Burg et al. (1997, 1998) traced sheared serpentinites and mafics around the rim of the massif, correlating these with the rocks from the India-Asia suture zone, together with fabrics in the underlying migmatitic basement to propose the general antiformal structure of the massif. They also report young fission track ages and U-Th-Pb ages for zircons at c 3-4 Ma – indicative of young cooling for the NBGPM. These results are broadly comparable with NPHM and prompted research to develop and quantify Zeitler et al.'s (2001) tectonic aneurysm model. These researches, chiefly using thermochronological data together with quantitative estimates of riverine stream power and landforms, have become somewhat polarized: do rivers and role in erosion and sediment transport control the sites of crustal deformation (e.g. Finnegan et al. 2008) or does the deformation happen anyway and is simply enhanced at sites of rapid erosion and sediment transport (e.g. King et al. 2016)?

The margins of the Namche Barwa – Gyala Peri Massif

Based on the interpretations of the structures of its margins, the NBGPM has been described as forming a promontory of the Indian continent, indenting the Lhasa Block (e.g. Koons 1995; Ding et al. 2001). The margins of the massif contain strongly sheared rocks of various tectonic affinities. The western margin is largely defined by the *Dongjui-Milin Shear Zone*, a left-lateral structure (Xu et al. 2012). It deforms two-mica peraluminous granites, the final part of the Gangdese batholith and related intrusions, in the vicinity of Loulan (Fig. 15). The granites are dated at 29-23 Ma (Pan et al. 2012). So the shear zone is presumably not a structure dating from the original collision of the Indian continent. Palin et al. (2015) report a composite history of shearing along the NW margin of the massif, based on U-Th-Pb geochronology. The earliest shearing

692 is dated at 23.9 ± 0.7 Ma, with continued ductile deformation continuing to c 8
693 Ma. The eastern margin of the NBGPM is also bounded by strike-slip wrench
694 shear – with right-lateral sense (Fig. 15) - variably termed the *Aniqiao-Mutuo* or
695 *Medog shear zone* (e.g. Dong and Xu 2016). The age of this structure is not
696 constrained by dated relationships with the Gangdese batholith. However, Dong
697 and Xu (2016) report U-Pb zircon ages from the synkinematic rims of zircons at
698 29.4-28.6 Ma.
699 The two margins, east and west, of the NBGPM show opposed-sense
700 wrench shear, but these bounding shear zones are considerably younger than
701 the age of original collision between the Indian continent and the Lhasa Block. In
702 this regard they may be similar to the Phuparash Shear Zone on the margins of
703 the NPHM, a similarly relatively late feature in Himalayan tectonics. However,
704 unlike NPHM, to date there are no structures described from the margins of the
705 NBGPM that are equivalent to the Liachar Thrust-Shahbatot Fault system,
706 discussed earlier, that accommodate the final part of the exhumation of the
707 Indian crust in the heart of the syntaxis. Quanru et al. (2006) report cataclastic
708 structures within the various bounding shear zones and infer that these are
709 extensional structures. However, an extensive, coherent brittle fault network has
710 yet to be described. Dong and Xu (2016) suggest shearing on the Medog shear
711 zone culminated at temperatures in excess of 350 C. Thus bounding shear zones
712 of the NBGPM developed at significant temperatures than those at NPHM and
713 appear to have been frozen in during exhumation of the massif, rather than have
714 evolved into shallow, cataclastic structures as at NPHM.
715
716 <u>Internal structure and metamorphism of the Namche Barwa – Gyala Peri Massif</u>
717
718 As at Nanga Parbat, the NBGPM contains crystalline basement units, presumed to
719 be derived from the Indian continent, which variably record a long and complex
720 metamorphic and deformational history. These include leucogranite seams,
721 though not as abundant as within the NPHM, dated as 3-10 Ma by Booth et al.
722 (2009). These authors also recognize four other magmatic events within the
723 NBGPM. Zhang et al. (2010) summarise metamorphic data for the massif. Garnet
724 pyroxenites from along the Tsangpo gorge SW of Namche Barwa peak (Fig. 15)

725 record granulite metamorphism with pressures of 1.8 – 1.4 GPa. These HP
726 granulites are preserved as dismembered pods within the Namche Barwa
727 Complex and yield U-Pb ages from zircon rims of 38-32 Ma. Thus rocks now
728 within the NBGPM were involved in thickening of the Indian continental crust at
729 an early stage in Himalayan tectonics. The cores of zircons yield Proterozoic ages
730 (Zhang et al. 2010), apparently clustering at 2.5 Ga, 1.6 Ga and 1.0 Ga. So, as at
731 NPHM, rocks of the NBGPM record a long and complex geological history.
732 Despite a few attempts to link geochronological and PT data deformation fabrics
733 along the marginal shear zones (e.g. Palin et al. 2915) this is not been done
734 within the massif as a whole. Tying in field relationships, including those
735 between deformation fabrics and intrusions, is important for creating a
736 mappable basement stratigraphy essential for relating structures to orogenic
737 processes.
738 Burg et al. (1997, 1998) present cross-sections displaying the general
739 antiformal structure of the massif and complex internal structure. However, the
740 vertical exaggeration (10:1) on their sections renders problematic the
741 interpretation of these structures. Booth et al. (2009) interpret the massif in
742 similar fashion to Burg et al. – with south-vergent asymmetric folds (Fig. 16a).
743 They also show a major shear zone that transects the massif just south of
744 Namche Barwa peak – the Namla Thrust (Fig. 16a). For these workers this is an
745 important structure that juxtaposes HT rocks in the north against lower-grade
746 metasediments in the south. Subsequent work, illustrated by Xu et al. (2012) has
747 modified this interpretation to include a series of tectonic slices, collectively
748 termed the Namche Barwa Complex (Fig. 16b, c). However, the Namla Thrust
749 retains a primary role in most models for the exhumation of the massif (see
750 Bracciali et al. 2016 for review), with Zeitler et al. (2014) likening it to the Rupal
751 Shear Zone at Nanga Parbat (as discussed above). Yet, as with the Rupal Shear
752 Zone, the Namla Thrust at outcrop appears to have acted exclusively as a
753 relatively high-temperature ductile structure. It is unclear how it might explain
754 the distribution of cooling ages derived from low-temperature
755 thermochronology.
756 Xu et al. (2012) report that the shear zones that contain the tectonic slices
757 of the Namche Barwa Complex show variable kinematics, with both southward

758 and northward-directed shear senses. They propose that these relationships
759 arise from pip-like exhumation of deeply buried Indian crust at around 40Ma.
760 This mechanism has been invoked in other orogenic belts, most clearly in the
761 Western Alps, to explain exhumation of eclogites through buoyancy-driven
762 processes (e.g. Chamenda et al. 1995). Xu et al. (2012) also indicate that the
763 Namche Barwa Complex is truncated against the bounding shear zones of the
764 massif truncate not only structures of the Namche Barwa Complex but also of
765 antiformal foliation trends in other parts of the massif. (Fig. 16b,c). These
766 structural relationships are consistent with the geochonological constraints on
767 the relative age of the various structures. Thus the exhumation of the NBGPM
768 active at present is only part of a protracted structural and thermal history of the
769 massif during Himalayan tectonics. This renders deductions of the geometric
770 relationships of the massif to the form of the original collision especially
771 problematic.
772
773 Thermochronology and active exhumation
774
775 The early studies of Burg et al. (1997) proposed that the Namche Barwa area had
776 been exhumed from depths of c 30 km in the past 4 Myr, at a time-averaged rate
777 of 7.5mm/yr. They compared this rate with fission track ages on zircon and
778 apatite together with U-Th-Pb ages on xenotime, thorite and zircon. From these
779 first data they argue for cooling rates of c 100 °C/Myr. In the past 20 years, Burg
780 et al.'s (1997) initial work has spawned considerable efforts to refine the overall
781 pattern, especially to establish the rates of down-cutting of the river gorges that
782 cross the massif. Finnegan et al. (2008) report unpublished Ar-Ar (biotite) ages
783 and a cluster of zircon fission track ages. Argon geochronology remains in
784 general use, although the challenge remains to discriminate radiogenic argon
785 inherited from basement degassing and thus to extract true cooling ages from
786 micas. However, the overall pattern of apparently young Ar-Ar mica ages are
787 consistent with results from an extensive variety of other thermochronological
788 methods.
789 Following syntheses by Stewart et al. (2008) and Zeitler et al. (2014),
790 recent results are collated and expanded by Tu et al. (2015), King et al. (2016)

and Yang et al. (2018). Samples from the Tsangpo gorge between the peaks of Gyali Peri and Namche Barwa, at elevations of c 2700m yield zircon (U-Th)/He ages of c 0.3 Ma (Stewart et al. 2008). Gneisses above the gorge (elevation of c 4 km) yield an apatite (U-Th-Sm)/He age of 1.5 ± 0.34 Ma (Yang et al. 2018). Tu et al. (2015) show that apatite fission track ages decrease with elevation up the flank of Namche Barwa peak. From this they conclude that enhanced Quaternary glaciation has driven increased exhumation rates. However, Yang et al. (2018) report ages along the Parlung as young as 0.18 ± 0.05 Ma for the apatite U-Th-Sm)/He system. They interpret the ages as the time samples cooled through 70 °C. It would appear then that denudation is especially rapid, exhuming recently cooled rocks through enhanced glaciation around the peaks and by rapid river down-cutting in the gorges.

Rather than use the thermochronological data to infer directly the cooling history for rocks of the eastern syntaxis, both King et al. (2016) and Yang et al. (2018) invert these data to test exhumation models. Both conclude that the locus of maximum denudation has migrated northwards through time. Within the spatial resolution of the existing samples, the current location of maximum rate of bedrock erosion lies just north of the outcrop of the NBGPM, along the Parlung river valley (Fig. 15). Presumably this in part reflects the capture of the Parlung drainage by the Tsangpo and the resultant rapid entrenchment of this drainage (e.g. Lang and Huntington 2014).

Attempts to deduce the record of denudation of the NBGPM during the Miocene have focused on the detrital record along the modern river valleys and within sedimentary basins south of the massif. Provenance studies based on detrital zircon U-Pb geochronology link source areas in the orogeny to ancestral foredeep (Siwalik) deposits of early Miocene and younger ages (Lang and Huntington 2014). These indicate that drainage from the Lhasa block flowed broadly across the Himalayas in the vicinity of the modern NBGPM from prior to the exhumation of the massif. Over time, and especially in the past 4 Myr, detritus from the NBGPM has increased in abundance. In modern sediments in the lower reaches of the Tsangpo river, over 50% is contributed from the massif, despite it accounting for >2% of the catchment (Bracciali et al. 2016).

824 The exhumation path

825

826 Zhang et al. (2015) summarise geochronological data within the context of the
827 metamorphism. Additional data are provided by Palin et al. (2015). These can be
828 linked to the low-temperature thermochronology discussed above. Bracciali et
829 al. (2016) report U-Pb rutile ages from the massif of 1.4 Ma – implying that
830 current bedrock was at 575 ± 75 C within the past 1-2 Ma. Syntheses stress the
831 complex, pulsed history of exhumation of the metamorphic rocks outcropping
832 along the margins and within the NBGPM. These results are summarized on Fig.
833 17. The challenge is to establish how far back the current tectonic regime, and its
834 exhumation path, stretch back into the geochronological record.
835 If there is short wavelength differential vertical motion in the continental
836 crust it should be manifest in the strain history and thus recorded by
837 deformation structures. Unlike NPHM – there have been no systematic attempts
838 to relate structures explicitly to the exhumation path, beyond definition of a few
839 ductile shear zones. What structures are responsible for the rapid exhumation?
840 Zeitler et al. (2014, following Booth et al. 2008) argue that the Nam La Thrust
841 together with the northern tectonic boundary of the massif define a pop-up
842 structure. As Bracciali et al. (2016) note, the current thermochronological data
843 are difficult to interpret tectonically in the absence of descriptions of the
844 structural geology of the massif. It is insufficient simply to assigning exhumation
845 histories, especially those that reference the last few km of denudation, to tracts
846 of gneisses thereby defining apparently distinct crustal blocks without also
847 determining the kinematics of the low-temperature fault zones that would be
848 required to bound them. As King et al. (2016) note and given the relief – perhaps
849 the thermochronological data are not charting bedrock tectonics at all but
850 merely the dynamic down-cutting associated with evolving drainage system.
851 Given the relief (> 6km) and steep near-surface geothermal gradient (>100
852 C/km), implicit in the low-temperature thermochronology, simply reorganizing
853 drainage can exhume rocks from temperatures approaching 600 °C without
854 invoking any specifically focused crustal thickening.

855

856 **Other syntaxes in the NW Himalayas**

Various loop-shaped map patterns have been identified in the NW Himalayas, including the Besham syntaxis (Coward et al 1988; Treloar et al. 1989) and other folded thrust systems (e.g. Greco and Spencer 1993). However, the most dramatic structure is the Hazara syntaxis (Fig. 18a), defined by the loop-shaped map pattern on the Main Boundary Thrust Zone. This structure straddles the *de facto* border between Pakistan and India making access especially difficult. Consequently there have been very few geological studies. Mapping and structural and stratigraphic data area provided by Bossart et al. (1988) and Greco and Spencer (1993), with stratigraphic data by Bossart and Ottiger (1989) and Critelli and Garzanti (1994). The general structure is an antiform, cored with Tertiary foredeep deposits of the Murree Formation. It is wrapped by thrust sheets that have been correlated with the Lesser Himalayan units to the SE (Greco and Spencer 1993), carried on the Main Boundary Thrust (Fig. 18a).

The Hazara syntaxis is generally interpreted to have formed by the superposition of the main Himalayan radial thrusting, here directed SW, upon the SSE-directed system in Pakistan (Coward et al. 1988). This has subsequently been supported by analyses of seismicity, including the devastating 2005 Kashmir earthquake (e.g. Avouac et al. 2006). Relocated aftershocks (Gibbons and Kvaerna 2017) define a buried continuation of the thrust NW of the Hazara syntaxis, leading to the Indus valley. The antiformal structure of the syntaxis is therefore readily interpreted to be the lateral tip fold to the Himalayan thrust front at depth (e.g. Coward et al. 1988).

The internal structure of the Hazara syntaxis is more complex than a simple antiform. The mapping of Bossart et al (1988; Fig. 18b) reveals a strongly asymmetric structure so that the axial trace of the antiform is located on the SW margin of the fold, with a prominent SE plunge. The northern plunge and NE limbv provides an exceptional stratigraphic section for the early Himalayan foredeep (Critelli and Garzanti 1994) that testify to the relatively low-relief of the early Himalayan chain. This changed so that by the early Miocene the foredeep was flooded with detritus, represented by the Siwaliks (see Burbank et al. 1996, for review). Unfolding the asymmetric anticline of the Hazara syntaxis reveals a lateral variation in the footwall to the Main Boundary Thrust. This

890 climbs section from west to east (Fig. 18c). The hangingwall also shows lateral
891 variation, with the Hazara Hills, to the west of the syntaxis, containing arrays of
892 heavily imbricated Phanerozoic supracrustals.
893 Structural mapping by Bossart et al. (1988) tracked cleavage through the
894 Hazara syntaxis. Strain studies reveal general flattening and the fabrics transect
895 the main anticline. These relationships demonstrate a significant component of
896 distributed strain to form the antiformal structure of the syntaxis – it does not
897 simply reflect differential uplift above a blind thrust (Fig. 18c). The strain
898 geometry is consistent with broadly NNW-SSE right lateral transpression.
899
900 **Discussion: Why syntaxes?**
901
902 There are various models for the structure of Himalayan syntaxes (Fig. 19). In
903 the aneurysm model (Zeitler et al. 2001; Fig. 19a), crustal structure is
904 represented by two opposed thrust shear zones with deformation apparently
905 focused by elevated near-surface temperatures and anatexis. There is a
906 coincidence of powerful rivers, high denudation and the location of the two main
907 syntaxial anticlines cored by the NPHM and NBGPM respectively. However, the
908 antiform of the Hazara syntaxis has formed but not amplified greatly. There are
909 no young metamorphic rocks in its core despite being crossed by large rivers
910 (Jhellum, Kaghan; Fig.18). Indeed the lateral continuity of the Hazara fold and its
911 zone of seismicity passes to the Indus river yet there is no significant uplift here.
912 So it appears that, although denudation, effective erosion of strength-supporting
913 “brittle” upper crust and the uplift of weaker, hot rocks towards the surface is an
914 effective softening mechanism for crustal deformation, the location of this
915 deformation must have tectonic origins.
916 There are various models proposed for the tectonic processes. Some of
917 these follow Zeitler et al. (2001) and argue that uplift of the NPHM and NBGPM is
918 fault-controlled. Synthesising studies of earthquake distributions at both
919 terminations of the Himalayan arc, Mukhopadhyay et al. (2011; Fig. 19b) depict
920 NPHM as an upper crustal pop-up and thrust-detachments beneath the Hazara
921 syntaxis. In contrast Butler et al. (2002; Fig. 19c) argue that widespread
922 distributed strain in the NPHM implies crustal-scale vertical stretching with

923 thrust faults simply accommodating failure in the residual brittle "lid" of the
924 massif. The pattern of distributed deformation in the Hazara syntaxis, reported
925 by Bossart et al. (1988) and discussed above further support this model.
926 Distributed deformation models broadly build from the crustal folding models
927 for the antiforms of the syntaxes (Burg and Podladchikov 1999, 2000) – although
928 they do not rely on maintaining strong layers within the crust to act as buckling
929 instabilities. Distributed crustal deformation is also invoked by Palin et al. (2012;
930 Fig. 19d) beneath the NBGPM, passing up onto margin faults. However, they
931 suggest normal faulting rather than thrusting to accommodate upper crustal
932 exhumation.
933 Other deformation models attempt to place the Himalayan syntaxes in a
934 larger tectonic context. Ding et al. 2001) propose a combination of two
935 processes. One involves folding of the mantling thrust structures to the NBGPM
936 and the other envisages indentation of the massif into the Lhasa Block (Fig 19e).
937 Replumaz et al. (2012; Fig. 19f) present the results of sandbox analogue
938 modeling using two opposed oblique backstops. They create convergent thrust
939 systems that, where they interfere at the convergent apex, create oblique folds.
940 The model configuration is explicitly designed to mimic the thrust systems of the
941 NW Himalayas and northern Pakistan and thus to explain the Hazara syntaxis
942 and NPHM. This setting is also the target of numerical modeling by Whipp et al.
943 (2014; Fig. 19g) that create orogeny-parallel flow. This results from partitioning
944 oblique convergence, as happens in the western Himalayas, creating excess
945 crustal thickening and rapid uplift at the NW termination of the oblique
946 convergence zone.
947
948 A model for the syntaxes
949 The contention here is that the tectonic origins of the antiforms that lie at
950 the heart of the Himalayan syntaxes should be investigated in their broader
951 context. Various large scale numerical simulations and regional observations
952 inform this context. Numerical simulations of the evolution of the crustal
953 thickness of Tibet using the thin viscous sheet approximation (reviewed by
954 Houseman and England 1996) generate crustal thickness maxima adjacent to the
955 corners of an assumed rigid Indian continental indenter. However, the rigidity of

the Indian indenter in these models means that crustal deformation is exclusively restricted to the northern side of the India-Asia suture. But what if the leading edge of the Indian continent is not rigid?

The near-perfect shape of the Himalayan arc (Bendick and Bilham 2001) suggests that crustal deformation within the Himalayas is best described, on a large-scale, as a ductile continuum rather than be the product of complex thrust stacking. Copley (2012) argues that the Himalayan arc is the product of gravity-driven flow of relatively low-viscosity crust onto higher-viscosity (effectively rigid) foreland. Distributed strain is a feature of the NPHM and the core of the Hazara antiform. This suggests that the two folds form along the NW lateral margin to a zone of ductile strain beneath the Himalayan arc to the SE (Fig. 20).

Most cross-sections through the Himalayas emphasise the continuity to depth of major thrust systems upon which displacements are strongly localised. Copley's (2012) model, adopted here (Fig. 20), suggests that the deep structure of the Himalayas is dominated by distributed strain. This dichotomy may be resolved if thrusting forms early and is being swept up by a southward-propagating strain wave. Copley (2012) considers the process to be a form of gravity spreading. The driver for this is most plausibly the overthickened continental crust of Tibet that is acting on the adjacent Indian crust, thickening this and collectively then driving further deformation out towards the foreland.

The timing of different parts of the tectonic history of the NPHM may be important here, within the Himalayan context. Even though India-Asia collision had occurred by c 52 Ma (see Green and Searle this volume), the main Himalayan syntaxes and their antiforms only formed within the past 10 Myr. First – the current juxtaposition of Kohistan arc on Indian crust was not achieved until the early Miocene – with movement on the Phuparash Shear Zone (Fig. 8) and it was from this configuration that the current tectonic regime developed. Given that, and the timing of high pressure in the Indian continental crust metamorphism dates to shortly after this time (Kouketsu et al. 2016), there is significant uncertainty as to the tectonic activity for the first half of Himalayan history (but see Treloar et al. this volume). It also renders linking the location of Himalayan syntaxes to the geometry of the Indian continent at the time of collision, and hence to original subduction geometry, especially uncertain. Nevertheless, the

989 leading edge of the Indian continental crust had been buried beneath the
990 southern edge of the Asian continent, presumably shortly after collision, as
991 recorded by the Kaghan eclogites (see Lanari et al. 2013). Peak temperatures of
992 650-750 C were achieved only after a further 20 Myr or longer, as is typical of
993 syn-orogenic (burial) metamorphism. Burial and radiogenic heating takes time
994 to warm and soften the Indian continental crust so that body forces created in
995 the thickened crust of Tibet are sufficient for it to yield. This means that the
996 Indian continent's Argand number (as discussed by Houseman and England
997 1996), which quantifies the ability of lithosphere to support buoyancy forces
998 against imposed lateral (tectonic) forces, must vary with time.
999 Relating the geological history of the NPHM to the deformation model
1000 presented here (Fig. 20) suggests that the modern extent of near perfect form of
1001 the topographic arc is a rather young attribute of the Himalayas. It has taken 10s
1002 Myr for sufficient volumes of the leading edge of the Indian continental crust to
1003 become soft enough and thus to deform through widespread distributed strain.
1004 This process is likely to be sensitive not only to the residence time of this crust
1005 beneath tectonic overburden but also to its intrinsic heat production and
1006 composition. It is interesting to note that the Himalayan arc does not define the
1007 northern extent of the Indian continent. In northern Pakistan, west of the
1008 syntaxes, there are major thrust systems that have stacked Indian continental
1009 crust and translated upper crust towards SSE (e.g. Coward et al. 1988). Likewise,
1010 Indian continental crust underlies the Assam syntaxis, east of the NBGPM. While
1011 these areas may be less susceptible to body forces transmitted from thickened
1012 Tibetan crust, it is also possible that both marginal areas beyond the syntaxes
1013 may be dominated by continental crust with lower heat production and thus
1014 have yet to warm sufficiently to deform by distributed crustal thickening.
1015
1016 **Conclusions**
1017
1018 The contribution has reviewed nearly four decades of geological research on the
1019 syntaxes at the two ends of the Himalayan arc, containing the Nanga Parbat-
1020 Haramosh massif and the Namche Barwa-Gyala Peri massif. Existing ideas and
1021 data have been discussed alongside their importance for understanding not only

1022 the early parts of the India-Asia collision but also how continental crust deforms
1023 in collision settings.
1024
1025 Nomenclature
1026 There is significant confusion in the literature, especially in the western syntaxis
1027 about nomenclature – following a redundant approach of naming tectonic
1028 contacts on the basis of the units they juxtapose. The bounding ductile shear
1029 zone to the NPHM juxtaposes the Indian continental crust against the Kohistan
1030 arc. But it is erroneous to call this the Main Mantle Thrust (c.f. Butler and Prior
1031 1988a and many others) as the contact is significantly younger than the MMT in
1032 its type area – it is a distinctly different structure - the Phuparash Shear Zone
1033 (Butler et al. 1992). Likewise, the tectonic contact along the western margin of
1034 the massif is sometimes conflated as a single "Raikhot Fault" (c.f. Madin et al.
1035 1989) – even though the margin (Butler et al. 1989) includes segments of the
1036 (probable) Phuparash Shear Zone, a top-NNW thrust-shear zone (the Liachar
1037 Thrust) and a major strike slip system (the Shahbatot Fault). Retaining imprecise
1038 terminology obscures consideration of the structural relationships that are
1039 essential for understanding the geological evolution of the region.
1040
1041 Early Himalayan history
1042 Both massifs comprise Indian continental crust that is juxtaposed against the
1043 southern margin of the northern Asian continent (the Kohistan arc in the west
1044 and the Lhasa Block in the east). Yet in neither case are these contacts the
1045 original suture: both were active several 10s Myr after collision. Earlier parts of
1046 the collision history are however recorded by both massifs. They contain rocks
1047 that originally resided in the Indian upper crust but which experienced HP
1048 metamorphic conditions relatively early in the Himalayan collision (at least 2.5
1049 GPa at NPHM, Lanari et al. 2013; 1.8 GPa for NBGPM, Zhang et al. 2010). Their
1050 exhumation to lower crustal depths broadly while the now over-lying Kohistan-
1051 Lhasa crust was intruded by mantle-sourced granitoids (George et al. 1993; Pan
1052 et al. 2012), remains poorly understood.
1053
1054 Active exhumation: which structures are responsible for the tectonics?

Much recent activity has been aimed at relating quantifying near-surface cooling histories using various thermochronological tools, feeding this into models of denudation, mountain uplift and riverine down-cutting. Near surface cooling rates of over 100 C/Myr are recorded in both massifs (Zeitler et al., 1982; Burg et al. 1997). However, relating tectonic geomorphology to crustal-scale deformation and metamorphic processes is challenging in poly-metamorphic terrains such as the two massifs. Only the later part of their long and complex history relates to exhumation and the modern expression of the massifs and the tectonic significance of many ductile structures is ambiguous. Thus the Rupal Shear Zone at Nanga Parbat is more plausibly a pre-exhumation structure so that a description of the massif's current structure as a pop-up is inaccurate (c.f. Schneider et al. 1999). Only the Liachar Thrust and shear zone (Butler & Prior 1988b; Butler 2000) shows the necessary combination of higher temperature shearing and cataclastic faulting. The exhumation is asymmetric, which accords the aneurysm model of Zeitler et al. (2001) as influenced by the distribution of rivers and erosion rates. Structures invoked in the eastern syntaxis to explain differential exhumation of the NBGPM have similar problems – illustrating the need for integrated structural mapping – admittedly difficult in the challenging landscape.

The aneurysm model: the role of melt overplayed?

Despite the acquisition of exceptional high-resolution thermo-chronological data, there remains significant uncertainty on how the feedbacks and coupling between rapid erosion, resultant decompression melting and deformation actually work. Existing understanding of strength-depth relationships in the crust certainly imply that exhumation of hot rocks causes weakening, reducing the depth to which frictional sliding operates ahead of temperature-dependent creep processes (e.g. Koons et al. 2002). The aneurysm model (Zeitler et al. 2001, Koons et al. 2002) takes this further by assuming that syn-kinematic melts, formed by erosion-promoted decompression, are agents of softening. This then focuses further deformation in shear zones into which melt has been emplaced. However, once crystallized, coarse-grained feldspar-rich rocks (e.g. leucogranites) are strong. Thus softening effects will only occur while granites

are still effectively liquid. The coincidence of granites in shear zones is insufficient evidence of this – the granite bodies should show evidence of weak inclusion behavior if they influenced deformation while liquid. This is not the case for the Liachar shear zone at Nanga Parbat: the leucogranites show strong inclusion behavior. However, unmigrated melt, forming grain boundary networks, may serve to weaken migmatites (e.g. Brown and Rushmer 1997; Crowley et al. 2009)) and these will be located in sites of rapid decompression with the appropriate reactants, not necessarily in active shear zones. Note however that these hot rocks will be weak anyway – compared with the load-bearing "brittle" (frictional sliding domain) upper crust so the effect of melt presence may be marginal rheologically. This discussion emphasizes the need for much more detailed investigation of crystallization rates vs deformation rates in deforming crust – an issue of far-greater impact than simply the tectonic evolution of the Himalaya syntaxes.

The aneurysm model: cause or effect?

Regardless of the specific softening mechanism, the aneurysm model suggests that surface processes are a primary control on the location of crustal deformation. Yet patterns of erosion and riverine down cutting derived from thermochronological data for the eastern syntaxis are not consistent with this model. (King et al. 2016) Furthermore, other crustal scale folds, such as the Hazara syntaxis have formed but not been amplified even though they are crossed by powerful rivers. At NPHM, the most rapid cooling rates are found in the north of the massif (Zeitler et al. 1982), where transected by the Indus gorge – yet the active structures here are dominated by strike-slip faults (Butler et al. 1989), not thrusts indicative of accelerated differential uplift. Thus the primary location and tectonic evolution of the main antiforms at the syntaxes appear not to be controlled by river systems. The feedback mechanisms implicit in the aneurysm model appear to be somewhat subdued, at least for these Himalayan examples.

A new tectonic model

Existing descriptions of the structure of the Himalayan syntaxes emphasise localized shear zones. However, both the NPHM and the Hazara examples show penetrative deformation fabrics (Bossart et al. 1988; Butler et al. 2002) that accommodate right lateral transpression. This is consistent with their location at the lateral edge to the Himalayan arc which is experiencing southward displacement (Coward et al. 1988). Distributed strains are unstudied in the NBGPM but might be predicted to accommodate left-lateral transpression.

It is proposed here that the exhumed distributed strain fabrics at NPHM are representative of the deformation style for the crust beneath the Himalayan arc. Distributed deformation at depth may then be propagating, with the Himalayan arc, southwards to the Indian foreland, in the manner proposed by Copley (2015), as a gravity current. Why this style of deformation is restricted laterally at the syntaxes is presently unclear. It may reflect lateral variations in the driving force or the propensity of the Indian continental crust to deform in this manner.

Quo vardis?

Despite the extensive research over recent years, albeit focused on eastern syntaxis, much more work is needed to address issues presented here. The challenges of tectonic geomorphology require more complete structural descriptions – tracing mapped and kinematically constrained structures from cataclastic fault zones into broader areas of distributed strain. There are abundant thermochronological tools to establish cooling histories down from 200 C. But tracing these histories into the structures demands direct dating of shear zone fabrics and intermediate temperature chronometers – a challenge given the constraints of isotopic systems, the very young and rapid rates of deformation and difficulties relating accessory phases to map-scale fabrics and kinematics. Building regional understanding is best served through establishing histories from integrated structural and metamorphic mapping at all scales. These are of course classic approaches in long-studied polymetamorphic terrains where relative geological histories were built – then calibrated by more elaborate geochronometers and petrology. Most of the data and compilations are open to many different interpretations – reflecting the uncertainty inherent in

much geological investigation. Consequently there remains considerable uncertainty in tectonic models for the Himalayan syntaxes and their constituent metamorphic massifs, including the one presented here.

Acknowledgements

I was introduced to the Himalayas by Mike Coward in the mid 1980s and remain indebted to him for inspiring a career studying orogenic tectonics. I also thank the numerous colleagues both from the UK and from Peshawar University who were companions on many field campaigns, especially around Nanga Parbat. Over the years this research has been variously supported by the UK's Natural Environment Research Council and the Royal Society. Finally I thank Peter Treloar for inviting this contribution and for his patience while I put it together.

References

Argles, T.W. 2000. The evolution of the Main Mantle Thrust in the western syntaxis. In: *Tectonics of the Nanga Parbat Syntaxis and the western Himalaya.* (eds M.A. Khan, P.J. Treloar, M.P. Searle and M.Q. Jan) Special Publications of the Geological Society, London, **170**, 101-122.

Argles, T.W. and Edwards, M.A. 2002. First evidence for Himalayan-age synconvergent extension recognized within the western syntaxis — Nanga Parbat, Pakistan. *Journal of Structural Geology,* **24**, 1327–1344.

Argles, T., Foster, G., Whittington, A., Harris, N. and George, M. 2003. Isotope studies reveal a complete Himalayan section in the Nanga Parbat syntaxis. *Geology,* **31**, 1109-1112.

Avouac, J-P. Ayoub, F., Leprince, S., JKonca, O. and Helmberger, D.V. 2006. The 2005, Mw 7.6 Kashmir earthquake: Sub-pixel correlation of Aster images and seismic waveforms analysis. *Earth and Planetary Science Letters,* **249**, 514-528.

Baig, M.S., Lawrence, R.D. and Snee, L.W. 1988. Evidence for late Precambrian to early Cambrian orogeny in northwest Himalaya, Pakistan. *Geological Magazine,* **125**, 83-86.

Beaumont, C., Fullsack, P. and Hamilton, J. 1992. Erosional control of active compressional orogens. In: *Thrust tectonics* (ed. K.R. McClay), Chapman and Hall, London, 1-18.

Bendick, R. and Bilham, R. 2001. How perfect is the Himalayan arc. *Geology*, **29**, 791-794.

Booth, A.L., Chamberlain, C.P., Kidd, W.S.F. and Zeitler, P.K. 2009. Constraints on the metamorphic evolution of the eastern Himalayan syntaxis from geochronologic and petrologic studies of Namche Barwa. *Geological Society of America Bulletin,* **121**, 385–407.

Bossart, P. and Ottiger, R. 1989. Rocks of the Murree Formation in northern Pakistan: indicators of a descending foreland basin of late Palaeocene to middle Eocene age. *Eclogae Geol. Helv.,* **82**, 133-165.

Bossart, P., Dietrich, D., Greco, A., Ottiger, R. and Ramsay, J.G. 1988. The tectonic structure of the Hazara-Kashmir Syntaxis, southern Himalayas, Pakistan. *Tectonics,* **7**, 273-297.

Bracciali, L., Parrish, R.R., Najman, Y., Smye, A., Carter, A. and Wijbrans, J.R. 2016. Plio-Pleistocene exhumation of the eastern Himalayan syntaxis and its domal 'pop-up. *Earth Science Reviews,* **160**, 350–385.

Brown, M. 2013. Granite: from genesis to emplacement. *Bulletin of the Geological Society of America,* **125**, 1079-1113.

Brown, M. and Rushmer, T. 1997. The role of deformation in the movement of granite melt: Views from the laboratory and the field. *In:* Holness, M.B., eds.,

Deformation-Enhanced Fluid Transport in the Earth's Crust and Mantle: The Mineralogical Society Series **8**, Chapman and Hall, London, 111–144.

Burbank, D.W., Beck, R.A. and Mulder, T. 1996. The Himalayan foreland basin. In: *The tectonic evolution of Asia*. (eds Yin, A. and Harrison, M.) Cambridge University Press, 149-188.

Burg, J.P. and Podladchikov, Y. 1999. Lithospheric scale folding: numerical modelling and application to the Himalayan syntaxes. *International Journal of Earth Science*, **88**, 190–200.

Burg, J.-P. and Podladchikov, Y. 2000. From buckling to asymmetric folding of the continental lithosphere: numerical modeling and application to the Himalayan syntaxes. In *Tectonics of the Nanga Parbat Syntaxis and the western Himalaya.* (eds M.A. Khan, P.J. Treloar, M.P. Searle and M.Q. Jan) Special Publications of the Geological Society, London, **170**, 219-236.

Burg, J.-P., Davy, P., Nievergelt, P., Oberli, F., Seward, D., Diao, Z., and Meier, M. 1997. Exhumation during folding in the Namche-Barwa syntaxis. *Terra Nova*, **9**, 53–56.

Burg, J.-P., Nievergelt, P., Oberli, F., Seward, D., Davy, P., Mauring, J.-C., Diao, Z., and Meier, M. 1998. The Namche Barwa syntaxis: Evidence for exhumation related to compressional crustal folding. *Journal of Asian Earth Sciences*, **16**, 239–252.

Butler, R.W.H. 2000. Structural evolution on the western margin of the Nanga Parbat massif, Pakistan Himalayas: insights from the Raikhot-Liachar area. In *Tectonics of the Nanga Parbat Syntaxis and the western Himalaya.* (eds M.A. Khan, P.J. Treloar, M.P. Searle and M.Q. Jan) Special Publications of the Geological Society, London, **170**, 51-75.

1250 Butler, R.W.H. and Prior, D.J. 1988a. Anatomy of a continental subduction zone: the
1251 Main Maintle thrust in Northern Pakistan. *Geol. Rundschau,* **77**, 239-255.
1252
1253 Butler, R.W.H. and Prior, D.J. 1988b. Tectonic controls on the uplift of Nanga Parbat,
1254 Pakistan Himalayas. *Nature*, **333**, 247-250.
1255
1256 Butler, R.W.H., Harris, N.B.W. and Whittington, A.G. 1997. Interactions between
1257 deformation, magmatism and hydrothermal activity during active crustal
1258 thickening: a field example from Nanga Parbat, Pakistan Himalayas. *Mineralogical*
1259 *Magazine*, **61**, 37-52.
1260
1261 Butler, R.W.H., Prior, D.J. and Owen, L.A. 1988. Flashfloods, earthquakes and uplift
1262 in the Pakistan Himalayas. *Geology Today*, **4**, 197-201.
1263
1264 Butler, R.W.H., Prior, D.J. and Knipe, R.J. 1989. Neotectonics of the Nanga Parbat
1265 syntaxis, Pakistan, and crustal stacking in the northwest Himalayas. *Earth and*
1266 *Planetary Science Lett*ers, **94**, 329-343.
1267
1268 Butler, R.W.H., Coward, M.P., Harwood, G.M. and Knipe, R.J. 1987. Salt control on
1269 thrust geometry, structural style and gravitational collapse along the Himalayan
1270 mountain front in the Salt Range of northern Pakistan. In: *Dynamical geology of salt*
1271 *and related structures* (ed. I. Lerche and J.J. O'Brien) pp. 339-418. Academic Press,
1272 Orlando.
1273
1274 Butler, R.W.H., George, M., Harris, N.B.W., Jones, C., Prior, D.J., Treloar, P.J. and
1275 Wheeler, J. 1992. Geology of the northern part of the Nanga Parbat massif, Northern
1276 Pakistan, and its implications for Himalayan tectonics. *Journal of the Geological*
1277 *Society, London,* **149**, 557-567.
1278
1279 Butler, R.W.H., Bond, C.E., Shipton, Z.K., Jones, R.R. and Casey, M. 2008. Fabric
1280 anisotropy controls faulting in the continental crust. *Journal of the Geological Society,*
1281 *London,* **165**, 449-452.
1282

Butler, R.W.H., Casey, M., Lloyd, G.E., Bond, C.E., McDade, P., Shipton, Z. and Jones, R. 2002. Vertical stretching and crustal thickening at Nanga Parbat, Pakistan Himalaya – a model for distributed continental deformation during mountain building. *Tectonics,* **21**, 10.1029/2001TC901022.

Carey, S.W. 1955. The orocline concept in geotectonics. *Papers and Proceedings of the Royal Society of Tasmania,* **89**, 255-288.

Chamenda, A.I., Mattauer, M., Malavielle, J. and Bokun, A.N, 1995. A mechanism for syn-collisional rock exhumation and associated normal faulting: results from physical modelling. *Earth and Planetary Science Letters,* **132**, 225-232.

Copley, A. 2012. The formation of mountain range curvature by gravitational spreading. *Earth and Planetary Science Letters*, **351-352**, 208-214.

Coward, M. P. 1985. A section through the Nanga Parbat syntaxis, Indus valley, Kohistan. *Geological Bulletin of the University of Peshawar,* **18**, 147-152

Coward, M.P. 1994. Inversion tectonics. In: *Continental deformation* (ed. Hancock, P.L.) Pergamon Press, Oxford, 289-304.

Coward, M.P., Butler, R.W.H., Chambers, A.F., Graham, R.H., Izatt, C.N., Khan, M.A., Knipe, R.J., Prior, D.J., Treloar, P.J. and Williams, M.P. 1988. Folding and imbrication of the Indian crust during Himalayan collision. *Philosophical Transactions of the Royal Society, London,* **A326**, 89-116.

Craw, D., Koons, P. O., Winslow, D., Chamberlain, C. P. and Zeitler, P. 1994. Boiling fluids in a region of rapid uplift, Nanga Parbat Massif, Pakistan. *Earth and Planetary Science Letters,* **128**, 169–182.

Critelli, S. and Garzanti, E. 1994. Provenance of the Lower Tertiary Murree redbeds (Hazara-Kashmir Syntaxis, Pakistan) and initial rising of the Himalayas. *Sedimentary Geology,* **89**, 265-284.

Crowley, J.L., Waters, D.J., Searle, M.P. and Bowring, A.S. 2009. Pleistocene melting and rapid exhumation of the Nanga Parbat massif, Pakistan: age and P-T conditions of accessory mineral growth in migmatite and leucogranite. *Earth and Planetary Science Letters,* **288**, 408-420.

Desio, A. 1964. *Geological tentative map of the western Karakorum*. Istituto Italiano d'arti grafiche, Bergamo.

DiBiase, R.A. 2014. River incision revisited. *Nature*, **505**, 294-295.

Ding, L., Zhong, D., Yin, A., Kapp, P. and Harrison, M. 2001. Cenozoic structural and metamorphic evolution of the eastern Himalayan syntaxis (Namche Barwa). *Earth and Planetary Science Letters*, **192**, 423-438.

Dong, H. and Xu, Z. 2016. Kinematics, fabrics and geochronology analysis in the Médog shear zone, Eastern Himalayan Syntaxis. *Tectonophysics*, **667**, 108-123.

Finlayson D.R., Montgomery, D.R. and Hallet, B. 2002. Spatial coincidence of rapid inferred erosion with young metamorphic massifs in the Himalayas. *Geology,* **30**, 219–222.

Finnegan, N.J., Hallet, B., Montgomery, D.R., Zeitler, P.K., Stone, J.O., Anders, A.M. and Liu, Y. 2008. Coupling of rock uplift and river incision in the Namche Barwa – Gyala Peri massif, Tibet. *Bulletin of the Geological Society of America,* **120**, 142-155.

Foster, G. Vance, D., Argles, T. and Harris, N. 2002. The Tertiary collision-related thermal history of the NW Himalaya. *Journal of Metamorphic Geology,* **20**, 827-843.

George, M.T., Harris, N.B.W. and Butler, R.W.H. 1993. The tectonic implications of contrasting post-collisional magmatism between the Kohistan island arc and the

1349 Nanga Parbat-Haramosh massif, Pakistan Himalaya. In: *Himalayan Tectonics* (ed.
1350 M.P. Searle and P.J. Treloar) Special Publications of the Geological Society, London
1351 **74**, 173-191.
1352
1353 Gibbons, S.J. and Kvaerna, T. 2017. Illuminating the seismicity pattern of the
1354 October 8, 2005, M = 7.6 Kashmir earthquake aftershocks. *Physics of the Earth and*
1355 *Planetary Interiors,* **270**, 1-8.
1356
1357 Greco, A. and Spencer, D.A. 1993. A section through the Indian Plate, Kaghan Valley,
1358 NW Himalaya, Pakistan. In: *Himalayan Tectonics* (ed. M.P. Searle and P.J. Treloar)
1359 Special Publications of the Geological Society, London **74**, 221-236.
1360
1361 Handy, M.R. 1999. Deformation regimes and the rheological evolution of fault
1362 zones in the lithosphere: the effects of pressure, temperature, grainsize and time.
1363 *Tectonophysics,* **163**, 119-152.
1364
1365 Hewitt, K. 2009. Catastrophic rock slope failures and late Quaternary
1366 developments in the Nanga Parbat - Haramosh Massif, Upper Indus basin,
1367 northern Pakistan. *Quaternary Science Reviews,* **28**, 1055-1069.
1368
1369 Hollister, L.S. and Crawford, M.L. 1986. Melt-enhanced deformation: a major
1370 tectonic process. *Geology,* **14**, 558-561.
1371
1372 Houseman, G. and England, P. 1996. A lithospheric-thicknening model for the
1373 Indo-Asian collision. In: *The tectonic evolution of Asia*. (eds Yin, A. and Harrison,
1374 M.) Cambridge University Press, 3-17.
1375
1376 Jouanne, F., Awan, A., Pecher, A., Kausar, A., Mugnier, J.L., Khan, A., Khan, N.A., and
1377 van Melle, J. 2014. Present-day deformation of northern Pakistan from Salt
1378 Ranges to Karakorum Ranges. *Journal of Geophysical Research: Solid Earth,* **19**,
1379 2487-2503.
1380

Khan, M.A., Treloar, P.J., Searle, M.P. and Jan, M.Q. (eds). 2000. *Tectonics of the Nanga Parbat Syntaxis and the Western Himalayas*. Geological Society, London, Special Publications **170**.

King, G.E., Herman, F. and Guralnik, B. 2016. Northward migration of the eatern Himalayan syntaxis revealed by OSL thermochronology. *Science*, **353**, 800-804.

Klootwijk, C.T., Conaghan, P.J. and Powell, C. McA. 1985. The Himalayan Arc: large-scale continental subduction, oroclinal bending and back-arc spreading. *Earth and Planetary Science Letters,* **75**, 167-183,

Koons, P.O. 1995. Modeling the topographic evolution of collision mountain belts. *Annual Review of Earth and Planetary Sciences,* **23**, 375-408.

Koons, P.O., Zeitler, P.K., Chamberlain, C.P., Craw, D. and Meltzer, A.S. 2002. Mechanical links between erosion and metamorphism in Nanga Parbat, Pakistan Himalaya. *American Journal of Science,* **302** – 749-773.

Kouketsu, Y., Hattori, K., Guillot, S. and Rayner, N. 2016. Eocene to Oligocene retrogression of the Stak eclogite in northwest Himalaya. *Lithos,* **240-243**, 155-166.

Lanari, P., Riel, N., Guillot, S., Vidal. O., Schwatz, S., Pêcher, A. and Hatton, K.H. 2013. Deciphering high-pressure metamorphism in collisional context using microprobe mapping methods: Application to the Stak eclogitic massif (northwest Himalaya). *Geology,* **41**, 111-114.

Lang, K.A. and Huntington, K.W. 2014. Antecedence of the Yarlung–Siang–Brahmaputra River, eastern Himalaya. *Earth and Planetary Science Letters,* **397**, 145–158.

Lawrence, R.D. and Ghauri A.A.K. 1983. Evidence for active faulting in Chilas District, N. Pakistan. *University of Peshawar Geological Bulletin,* **10**, 185-186.

Leland, J., Reid, M.R., Burbank, D.W., Finkel, R. and Caffee, M. 1998. Incision and differential bedrock uplift along the Indus River near Nanga Parbat, Pakistan Himalaya, from ^{10}Be and ^{26}Al exposure age dating of bedrock straths. *Earth and Planetary Science Letters,* **154**, 93-107.

Madin, I. P., Lawrence, R. D. and Ur-Rehman, S. 1989. The northwestern Nanga Parbat-Haramosh massif; evidence for crustal uplift of the northwestern corner of the Indian craton. *In: Tectonics of the Western Himalayas* (eds. Malinconico, L. L. and Lillie, R. J.) Geological Society of America. Special Paper **232***,* 169-1 82.

Marshak, S. 1988. Kinematics of orocline and arc formation in thin-skinned orogens. *Tectonics,* **7**, 73-86.

Meltzer, A., Sarker, G., Beaudoin, B., Seeber, L. and Armbruster, J. 2001. Seismic characterization of an active metamorphic massif, Nanga Parbat, Pakistan Himalaya. *Geology,* **29**, 651–654.

Misch, P. 1949. Metasomatic granitization of batholithic dimensions. *American Journal of Science,* **247**, 209-245.

Mukhopahyay B., Acharyya, A., Bhattacharyya, D., Dasgupta, S. and Pande, P. 2011. Seismotectonics at the terminal ends of the Himalayan arc. *Geomatics, Natural Hazards and Risk,* **2**, 159-181.

Neves, S.P., Vauchez, A., Archanjo, C.J. 1996. Shear zone-controlled magma emplacement or magma-assisted nucleation of shear zones? Insights from northeast Brazil. *Tectonophysics,* **262**, 349-364.

Palin, R.M., Searle, M.P., St Onge, M.R., Waters, D.J., Roberts, N.M.W., Horstwood, M.S.A., Parrish, R.R., Weller, O.M. 2015. Two-stage cooling history of politic and semi-pelitic mylonite (sensu lato) from the Dongjiu-Milin shear zone, northwest flank of the eastern Himalayan syntaxis. *Gondwana Research* **28**, 509-530.

Pan, F-B., Zhang, H-F., Harris, N., Xu, W-C. and Guo, L. 2012. Oligocene magmatism in the eastern margin of the east Himalayan syntaxis and its implication for the India–Asia post-collisional process. *Lithos* **154**, 181-192.

Park, S. and Mackie, R. 2000. Resistive (dry?) lower crust in an active orogen, Nanga Parbat, northern Pakistan. *Tectonophysics,* **316**, 359–380.

Passchier, C.W., Mancktelow, N.S. and Grasemann, B. 2005. Flow perturbations: a tool to study and characterise heterogeneous deformation. *Journal of Structural Geology*, **27**, 1011-1026.

Poage, M.A., Chamberlain, C.P. and Craw, D. 2000. Massif-wide metamorphism and fluid evolution at Nanga Parbat, Northern Pakistan. *American Journal of Science,* **300**, 463–482.

Pognante, U., Benna, P. and Le Fort, P. 1993. High-pressure metamorphism in the High Himalayan crystallines of the Stak valley, northeastern Nanga Parbat-Haramosh syntaxis, Pakistan Himalaya. In *Himalayan Tectonics* (ed. M.P. Searle and P.J. Treloar) Special Publications of the Geological Society, London **74**, 161-172.

Quanru, G., Guitang, P., Zheng, L., Chen, Z., Fisher, R.D., Sun, Z., Ou, C., Dong, H., Wang, X., Li, S., Lou, X. and Fu, H. 2006. The Eastern Himalayan syntaxis: major tectonic domains, ophiolitic mélanges and geologic evolution. *Journal of Asian Earth Sciences,* **27**, 265-285.

Rai, S.S., Priestley, K., Gaur, V.K., Mitra, S., Singh, M.P. and Searle, M. 2006. Configuration of the Indian Moho beneath the NW Himalaya. *Geophysical Research Letters,* **33**, L15308.

Replumaz, A., Vignon, V., Regard, V., Martinod, J. and Guerrero, N. 2012. Eaast-west shortening during north-south convergence, example of the NW Himalayan

syntaxis. *Australian Journal of Earth Sciences*, **59**, 845-858.

Schneider, D.A., Edwards, M.A., Kidd, W.S.F., Khan, M.A., Seeber, L. and Zeitler, P.K., 1999. Tectonics of Nanga Parbat,western Himalaya: synkinematic plutonism within doubly vergent shear zones of a crustal-scale pop-up structure. *Geology,* **27**, 999–1002.

Schneider, D.A., Zeitler, P.K., Kidd, W.S.F. and Edwards, M.A. 2001. Geochronologic constraints on the tectonic evolution and exhumation of Nanga Parbat, Western Himalaya, revisited. *Journal of Geology,* **109**, 563–583.

Shroder, J.F., Jr., and Bishop, M.P. 2000. Unroofing of the Nanga Parbat Himalaya. In *Tectonics of the Nanga Parbat Syntaxis and the western Himalaya.* (eds M.A. Khan, P.J. Treloar, M.P. Searle and M.Q. Jan) Special Publications of the Geological Society, London, **170**, 163–179.

Sibson, R.H. 1983. Continental fault structure and the shallow earthquake source. *Journal of the Geological Society, London,* **140**, 741-767.

Stewart, R.J., Hallet, B., Zeitler, P.K., Malloy, M.A., Allen, C.M. and Trippett, D. 2008. Brahmaputra sediment flux dominated by highly localized rapid erosion from the easternmost Himalaya. *Geology,* **36**, 711.

Tahirkheli, R.A.K. and Jan, M.Q. (eds) 1979. Geology of Kohistan, Karakoram Himalaya, Northern Pakistan. *Geological Bulletin of the University of Peshawar*, **11**, pp. 187.

Tiwari, V.M., Mishra, D.C. and Pandey, A.K. 2015. The lithospheric denisity structure below the western Himalayan syntaxis: tectonic implications. In *Tectonics of the Himalaya.* (eds S. Mukherjee, R. Carosi, P.A. van der Beek, B.K. Mukherjee and D.M. Robinson) Special Publications of the Geological Society, London, **412**, 55-65.

1513 Treloar, P.J., Broughton, R.D., Williams, M.P., Coward, M.P. and Windley, B.F.
1514 1989. Deformation, metamorphism and imbrication of the Indian plate, south of
1515 the Main Mantle Thrust, north Pakistan. *Journal of Metamorphic Geology,* **7**, 111-
1516 125.
1517
1518 Treloar, P.J., George, M.T. and Whittington, A.G. 2000. Mafic sheets from Indian
1519 plate gneisses in the Nanga Parbat syntaxis: their significance in dating crustal
1520 growth and metamorphic and deformation events. In: *Tectonics of the Nanga*
1521 *Parbat Syntaxis and Western Himalaya* (eds. Khan, M.A., Treloar, P.J., Searle, M.P.,
1522 Jan, M.Q.), Geological Society of London Special Publication **170**, pp. 25–50.
1523
1524 Tu, J.-Y., Ji, J.-Q., Sun, D.-X., Gong, J.-F., Zhong, D.-L. and Han, B.-F. 2015. Thermal
1525 structure, rock exhumation, and glacial erosion of the Namche Barwa Peak,
1526 constraints from thermochronological data. *Journal of Asian Earth Sciences,* **105**,
1527 223–233.
1528
1529 Wadia, D.N. 1919. *The geology of India*. Macmillan and Co., London
1530
1531 Warren, C.J., Smye, A.J., Kelley, S.P. and Sherlock, S.C. 2012. Using white mica
1532 40Ar/39Ar data as a tracer for fluid flow and permeability under high-P
1533 conditions; Tauern Window, Eastern Alps. *Journal of Metamorphic Geology,* **30**,
1534 63–80.
1535
1536 Webb, A.A.G. 2013. Preliminary balanced palinspastic reconstruction of Cenozoic
1537 deformation across the Himachal Himalya (northwest India). *Geosphere,* **9**, DOI:
1538 10.1130/GES500787.1
1539
1540 Wheeler, J., Treloar, P.J. and Potts, G.J. 1995. Structural and metamorphic
1541 evolution of the Nanga Parbat syntaxis, Pakistan Hima layas, on the Indus gorge
1542 transect: the importance of early event. *Geological Journal,* **30**, 349-371.
1543

Whipp, D.M., Beaumont, C. and Braun, J. 2014. Feeding the "aneurysm": Orogen-parallel mass transport into Nanga Parbat and the western Himalayan syntaxis. *Journal of Geophysical Research: Solid Earth*, **119**, 5007-5096.

Whittington, A.G. 1996. Exhumation over-rated at Nanga Parbat, northern Pakistan. *Tectonophysics,* **260**, 215-226.

Whittington, A.G. and Treloar, P.J. 2002. Crustal anatexis and its relation to the exhumation of collision orogenic belts, with particular reference to the Himalaya. *Mineralogical Magazine,* **66**, 53-91.

Whittington, A.G., Harris, N.B.W. and Butler, R.W.H., 1999. Contrasting anatectic styles at Nanga Parbat, northern Pakistan. In: *Himalaya and Tibet: Mountain Roots to Mountain Tops* (eds. Macfarlane, A., Sorkhabi, R.B., Quade, J.), Geological Society of America Special Paper **328**, 129–144.

Whittington, A., Harris, N.B.W., Ayres, M.W. and G. Foster, G. 2000. Tracing the origins of the western Himalaya: an isotopic comparison of the Nanga Parbat massif and Zanskar Himalaya. in *Tectonics of the Nanga Parbat Syntaxis and the Western Himalaya* (eds M.A. Khan, P.J. Treloar, M.P. Searle and M.Q. Jan) Special Publications of the Geological Society, London, **170**, 210-218.

Willett, S. D. 1999. Orogeny and orography: the effects of erosion on the structure of mountain belts. *Journal of Geophysical Research, Solid Earth,* **104**, 28957-28981.

Xu, Z., Ji, S., Cai, Z., Zeng, L., Geng, Q. and Cao, H. 2012. Kinematics and dynamics of the Namche Barwa Syntaxis, eastern Himalaya: constraints from deformation, fabrics and geochronology. *Gondwana Research,* **21**, 19–36.

Yang, R., Herman, F., Fellin, M.G. and Maden, C. 2018. Exhumation and topographic evolution of the Namche Barwa Syntaxis, eastern Himalaya. *Tectonophysics,* **722**, 43-52.

1577
1578 Zeitler, P.K. 1985. Cooling history of the NW Himalaya, Pakistan. *Tectonics,* **4**,
1579 127-151.
1580
1581 Zeitler, P.K., Johnson, N.M., Naeser, C.M. and Tahirkheli, R.A.K. 1982. Fission-track
1582 evidence for Quaternary uplift of the Nanga Parbat region, Pakistan. *Nature,* **298**,
1583 255-257.
1584
1585 Zeitler, P.K., Sutter, J. F., Williams, I. S., Zartman, R. and Tahirkheli, R. A. K. 1989
1586 Geochronology and temperature history of the Nanga Parbat-Haramosh Massif,
1587 Pakistan. *In: Tectonics of the Western Himalaya* (eds. Malinconico, L. L. and Lillie,
1588 R. J .) Geological Society of America Special Paper **232**, 1-22.
1589
1590 Zeitler, P.K., Chamberlain, C. P. and Smith, H. A. 1993. Synchronous anatexis,
1591 metamorphism and rapid denudation at Nanga Parbat (Pakistan Himalaya).
1592 *Geology,* **21**, 347-350.
1593
1594 Zeitler, P.K., Koons, P.O. and Bishop, M.P. et al. 2001. Crustal reworking at Nanga
1595 Parbat, Pakistan: Metamorphic consequences of thermo-mechanical coupling
1596 facilitated by erosion. *Tectonics,* **20**, 712–728.
1597
1598 Zeitler, P.K., Meltzer, A.S., Koons, P.O., Craw, D., Hallet, B., Chamberlain, C.P., Kidd,
1599 W.S.F., Park, S.K., Seeber, L., Bishop, M. and Schoder, J. 2001. Erosion, Himalayan
1600 geodynamics and the geomorphology of metamorphism. *GSAToday,* **11**(1), 4-9.
1601
1602 Zeitler, P.K., Meltzer, A.S., Brown, L., Kidd, W.S.F., Lim, C. and Enkelmann, E. 2014.
1603 Tectonics and topographic evolution of Namche Barwa and the easternmost
1604 Lhasa block, Tibet. *Spec. Pap. Geol. Soc. Am,.* **507**, 23–58.
1605
1606 Zhang, Z.M., Zhao, G.C., Santosh, M., Wang, J.L., Dong, X. and Liou, J.G. 2010. Two-
1607 stages of granulite-facies metamorphism in the eastern Himalayan syntaxis,
1608 south Tibet: petrology, zircon geochronology and implications for the subduction
1609 of Neo-Tethys and the Indian continent beneath Asia. *Journal of Metamorphic*

Geology, **28**, 719–733.

Zhang, Z., Dong , X., M. Santosh, M., Liu, F., Wang, W., Yiu, F., He, Z. and Shen, K. 2012. Petrology and geochronology of the Namche Barwa Complex in the eastern Himalayan syntaxis, Tibet: Constraints on the origin and evolution of the north-eastern margin of the Indian Craton. *Gondwana Research,* **21**, 123-137.

Zhang, Z., Xiang, H., Dong, X., Ding, H. and He, Z. 2015. Long-lived high-temperature granulite facies metamorphism in the Eastern Himalayan orogeny, south Tibet. *Lithos,* **212-215**, 1-15.

Figure captions

Figure 1. Location map for the Himalayan syntaxes. Modified after Webb (2013). Boxed areas: a – Fig. 3; b – Fig. 15; c – Fig. 18a).

Figure 2. Analysis of publications (peer-reviewed in international journals) grouped in two-year sample windows based on a search using GoogleScholar (October 2017) using the terms "Nanga Parbat massif" and "Namche Barwa massif", filtered to show only those results based on geological/ geomorphological field research. The peak in the Nanga Parbat results marks the publication of Geological Society Special Publication 170 (Khan et al. 2000).

Figure 3. Simplified geological map of the Nanga Parbat – Haramosh massif, re-interpreted from existing mapping (Butler et al. 1992, 2000; Schneider et al. 2001).

Figure 4. Photographs of the NPHM. a) looking south to Nanga Parbat from the ridge east of Darchan village (Fig. 3) showing the relief across the syntaxis. b) Rupal face and glacier. c) looking north up the Indus valley on the western flank of NPHM from above the mouth of the Raikhot valley (Fig. 3). d) looking down along the Indus gorge near Shengus village. e) aerial photograph (from c 5000m) looking to the summit of Nanga Parbat (slightly cloud-obscured) with Chongra in the foreground. f) aerial photograph of the west ridge of Haramosh. Note the layered series of rocks inclined to ESE on the summit right of the mountain.

Figure 5. Basement stratigraphy and rock-types for the Nanga Parbat Haramosh Massif. a) Interpreted rock relationships (unscaled); b) amphibolites in marbles, intrerptreted as a Tethyan cover succession with meta-basic intrusions, deformed into recumbent fold, Sassi area, Indus gorge (cliff height c 50m, looking west); c) metabasic intrusion cross-cutting ore-existing migmatitic fabric, both subsequently deformed. Indus gorge (compass scale); d) typical migmatites from the heart of the NPHM, fabrics probably of early Proterozoic age (Tato village, compass scale); e) biotite granite (with metasediment xenolith) from the upper

Rupal glacier (pencil is c 15 cm long); f) view onto intrusive relationships of biotite granite across non-migmatitic metasediments (Tarshing Group of Butler et al. 2000 – visible cliff height c 1200m).

Figure 6. The structure of the Phuparash Shear Zone, the ductile shear zone that juxtaposes the Kohistan arc against rocks of the Indian continent and commonly misrepresented as the Main Mantle Thrust (cf Butler and Prior 1988a). a) Seen in cliff section on the south wall of the Phuparash peaks (visible cliff height c 2500m). b) in the south wall of the Indus gorge on the eastern margin of the NPHM (visible cliff height c 300m). c) sketch section (after Butler and Prior 1988a) summarizing structural relationships in the Indus gorge on the western margin of the NPHM which demonstrate top-SSE shear sense. d) large-scale form of deformed granite sheets – the final magmatic component of the Kohistan arc. The visible cliff height is c 250m. e) high strained part of the Phuparash shear zone with strongly attenuated granite sheets. Coin for scale. f) Asymmetrically boudinaged mafic sills within marbles, part of the "cover" series of the NPHM.

Figure 7. PT conditions paired in distance across the Nanga Parbat Haramosh Massif. a and b show transects for the Astor valley and Raikhot-Chongra-Astor village respectively (data from Poage et al. 2000). c) shows general PT-constraints for the massif, using the HP-LT conditions preserved in the Stak eclogites (Lanari et al. 2013) and the HT-LP conditions preserved in the upper Raikhot valley (Crowley et al. 2009).

Figure 8. Scaled schematic cross-sections showing the evolution (a-b in time) for the pre-exhumation history of the Nanga Parbat Haramosh Massif and its relationship to the Kohistan arc terrain. Compare the relative position of markers x, y and z. x – the current location of the hangingwall to the Phuparash shear zone in the Haramosh area. y – the eclogitic rocks (and their retrogressed equivalents) of the Indian continental crust . z – the leading edge of lower crust of the Kohistan arc – former hangingwall to the Main Mantle Thrust, now hidden by the overstepping Phuparash Shear Zone.

Figure 9. Competing interpretations of the internal structure of the Nanga Parbat – Haramosh Massif shown on cross-sections. a) shows the composite antiformal structure preserved along the Indus gorge deduced by Wheeler et al. (1995). b) illustrates the geometry of the Liachar Thrust and shear zone interpreted by Butler et al. (1988), based on a transect through Raikhot to Astor. c) Schneider et al.'s (2001) cross-section through the southern part of the massif illustrating the "pop-up" structure proposed by Schneider et al. (1999).

Figure 10. Field relationships of exhumation-related granites in the Nanga Parbat Haramosh Massif. a) the Jutial leucogranite pluton – equant feldspar-quartz – tourmaline granite, with margins discordant to host gneisses. b) far-migrated leucogranite pegmatites from the Indus gorge forming discordant sills, indicative of vertical stretching. c) locally sourced diffuse-margin leucogranite seams preferentially developed in boudin necks (Tato area). d) cordierite-bearing leucogranite seams forming web-arrays in boudin necks. The remaining images are from leucogranite pegmatites in the Liachar shear zone, lower Raikhot valley. e) apparently deformed pegmatite, cross-cutting sheared migmatitic gneisses and amphibolites. f) deflected pegmatite g) compositionally zoned margin to the pegmatite dismembered into the shear zone indicating structurally controlled fractional crystallization of the original melt. h) typical coarsely-crystalline but undeformed igneous texture within the pegmatite. i) folded pegmatite with coarse margin facies and deformed, quartz-rich interior facies (j).

Figure 11. Fission track profile across the Nanga Parbat Haramosh Massif along the Indus gorge transect (diagram after Butler et al. 1989; data from Zeitler et al. (1982)).

Figure 12. Exhumation-related deformation on the western margin of the Nanga Parbat Haramosh Massif, in the Raikhot valley and surroundings. a) cross-section showing deformation kinematics. b) the Liachar Thrust in its type locality, c 5 km NE of Raikhot Bridge (hillside c 2 km high). c) the lower Raikhot gorge, showing

a section through the Liachar Shear Zone. Main cataclastic fault indicated by pecked line. d) asymmetric feldspar augen and s-c fabrics in orthogneiss showing top-NW shear sense. e) symmetric feldspar augen (indicative of quasi-pure shear sub-vertical stretching) in orthogneiss in footwall to the Liachar thrust zone. f) conjugate shear zones (with local leucosome patches) developed in migmatites at Tato village.

Figure 13. Revised cross-section through the Nanga Parbat – Haramosh Massif.

Figure 14. Temperature-depth plot for the heart of the Nanga Parbat – Haramosh Massif. Inset: Strength-depth plot for the NPHM – based on interacting depth- and temperature-dependent deformation mechanisms. See text for information.

Figure 15. Simplified geological map of the Namche Barwa – Gyala Peri massif, modified after Booth et al. 2009. The zone of HP-UHP granultes is after Xu et al. (2012). The zone of maximum bedrock erosion is after King et al. (2016). The lines of section (A-A'; B-B'; C-C') are those shown in Fig. 16.

Figure 16. Cross-sections through the Namche Barwa – Gyala Peri massif (lines of section on Fig. 15). a) A-A': after Booth et al. (2009). b) B-B' and c) C-C' are after Xu et al. (2012).

Figure 17. Temperature-depth-time plots for rocks within the Namche Barwa – Gyala Peri massif, with data from Zhang et al. (2015). The numbers are ages of various parts of the paths. The two paths (green boxes, grey ellipse) are recorded by different parts of the "Namche Barwa gneisses" but the relationship between these sites is obscure.

Figure 18. a) Simplified sketch map of the thrust systems in the NW Himalayas. Overlain with the pattern of after-shocks, simplified from the analysis by seismicity Gibbons and Kvaerna (2017). b) Geological map of the Hazara syntaxis (simplified from Bossart et al. 1988). c) Fold model for Hazara syntaxis and

1753 lateral tip to frontal thrust, illustrated on a schematic SW-NE cross-section
1754 approximately through the city of Muzaffarabad. MBT- Main Boundary Thrust.
1755
1756 Figure 19. A review of models for the syntaxial anticlines (scales and
1757 orientations, or lack thereof, are after those shown by the source publication). a)
1758 the aneurysm model of Zeitler et al. (2001) relating erosion and sediment
1759 evacuation by rivers to enhanced exhumation, elevated near-surface
1760 temperatures and the consequent localization of deformation. b) Mukhopahyay
1761 et al.'s (2011) block model to show the relationship between the NPHM, Hazara
1762 syntaxis and earlier thrusts (MMT – Main Mantle Thrust, MBT – Main Boundary
1763 Thrust) together with their younger subsurface structure (RF – "Raikhot Fault").
1764 c) The distributed deformation model of Butler et al. (2002) for the crustal
1765 structure beneath NPHM, seen in cross-section. d) Palin et al.'s (2015) cross-
1766 section interpretation of the relationship between crustal thickening beneath
1767 NBGPM and the major Himalayan thrust and shear zones (STD – South Tibetan
1768 Detachment, MCT – Main Central Thrust, MBT – Main Boundary Thrust, MFT –
1769 Main Frontal Thrust). e) Ding et al.'s (2001) model in plan-view for the
1770 indentation of the Asian continent (Lhasa Block) by the NBGPM that forms a
1771 promontory of the Indian continent. f) plan-view sketch based on the
1772 photographs of analogues experiments by Replumaz et al. (2012) showing
1773 antiform formation at the apex between convergent thrust systems. The brown
1774 lines formed an orthogonal grid before deformation and illustrate rotational
1775 strain. g) Output (plan-view) from numerical modeling of partitioned oblique
1776 convergence by Whipp et al. (2014).
1777
1778 Figure 21 – Schematic block diagram, viewed looking SW to show the
1779 interpretation presented here for the western syntaxes as the lateral edge to the
1780 Himalayan crustal gravity current proposed by Copley (2012). The thermal
1781 structure is illustrative and qualitative. Note that displacement on the Main
1782 Frontal Thrust passes back down dip into ductile strain accommodating vertical
1783 stretching and crustal shortening. This forms the leading edge of the ductile
1784 component to the gravity current. Right lateral compression characterizes the
1785 deep structure of the syntaxes, as exhumed within the NPHM.

Figure 1

Click here to download Figure Fig 1 locationmap.pdf

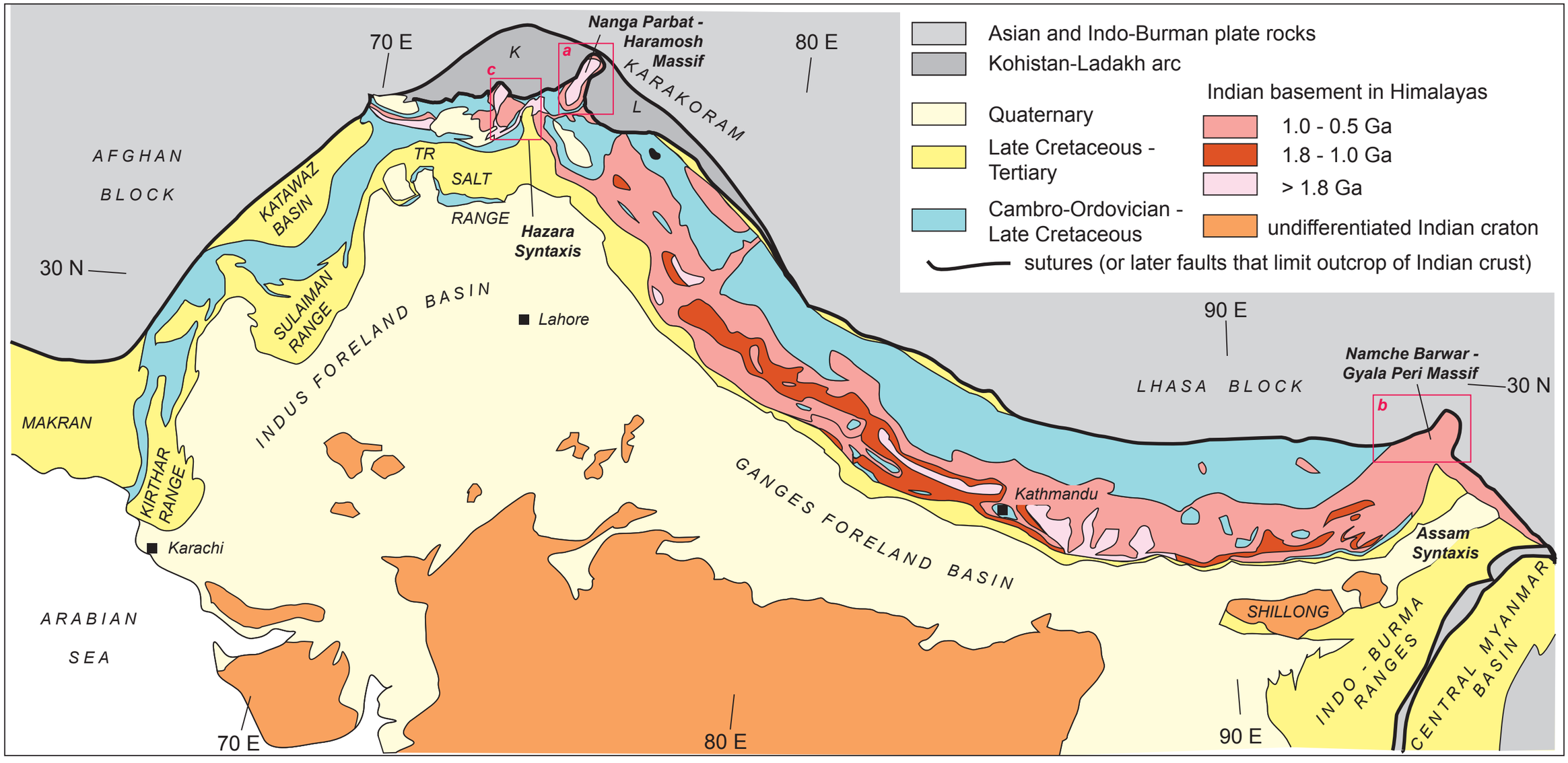

Figure 2

Click here to download Figure Fig 2 literature by year.pdf

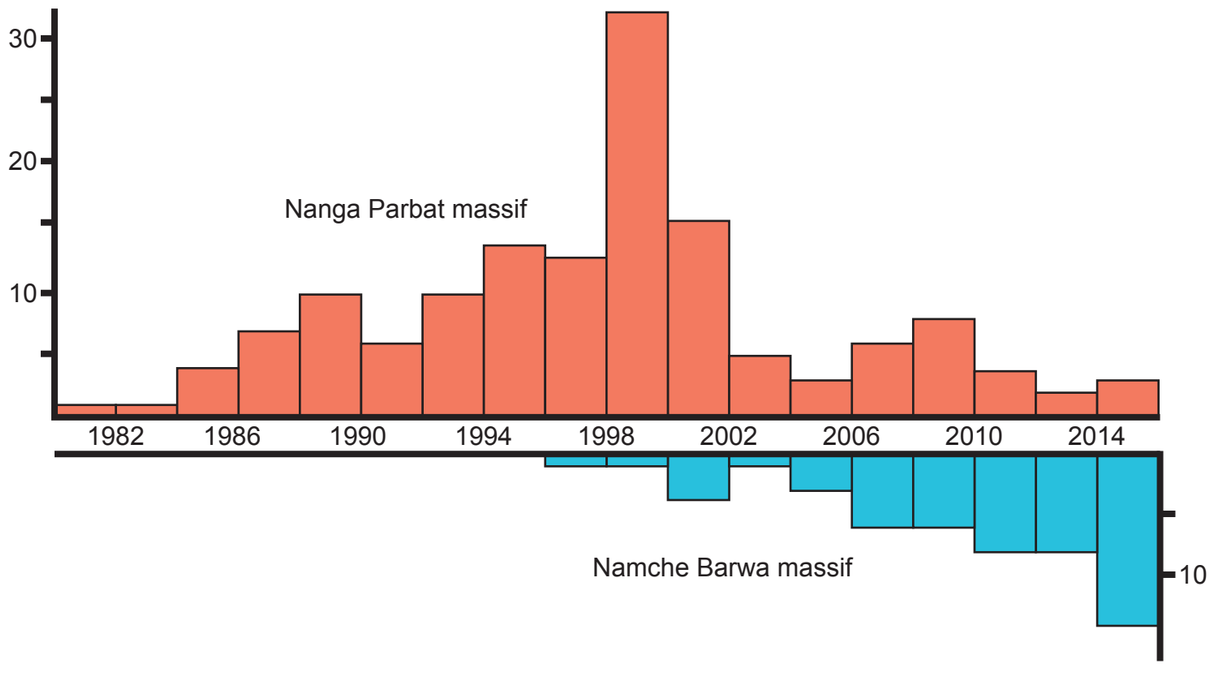

Figure 3

Click here to download Figure Fig 3 NPHMmap.pdf

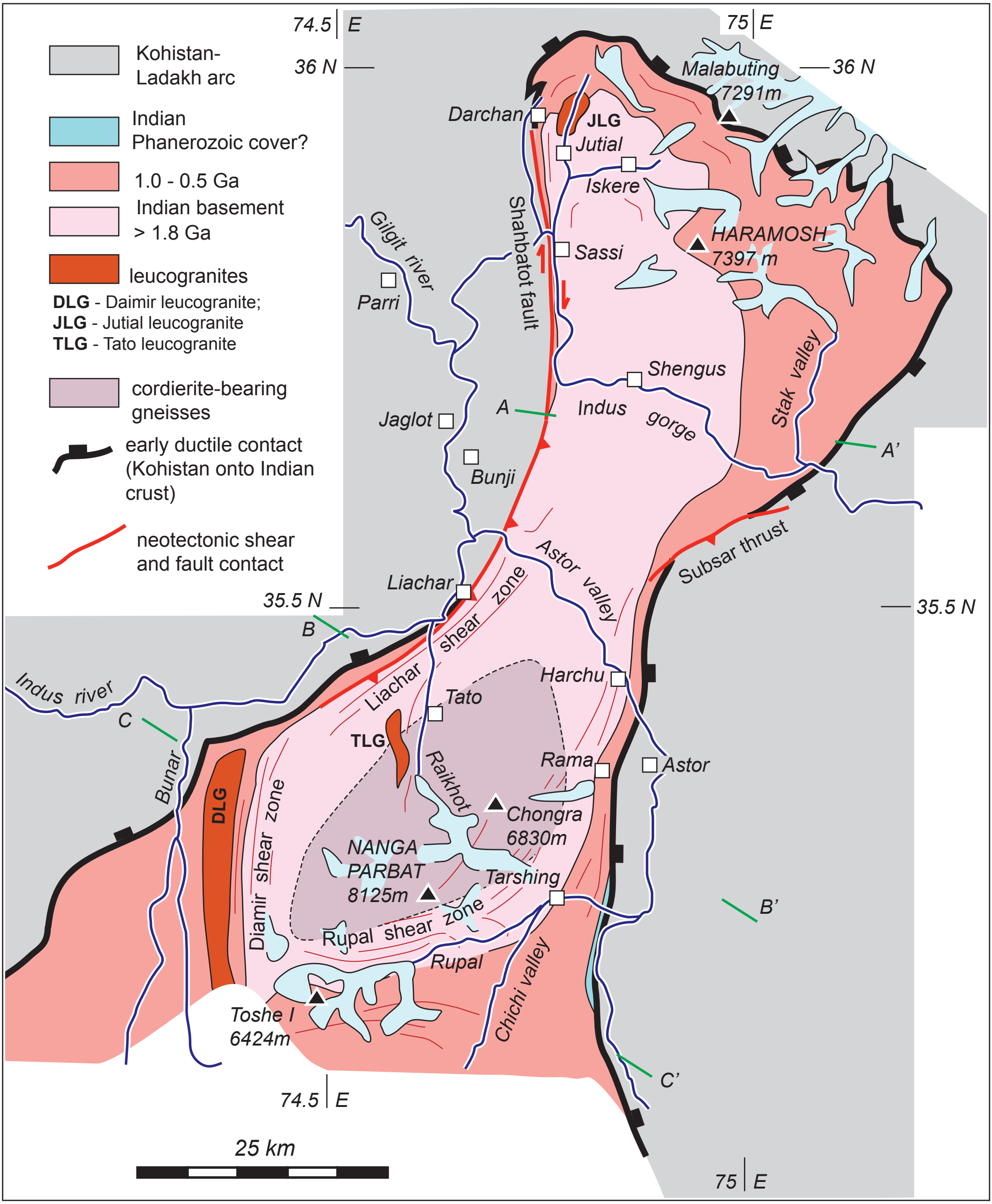

Figure 4A

Click here to download Figure Fig 4a NPHM photos a.jpg

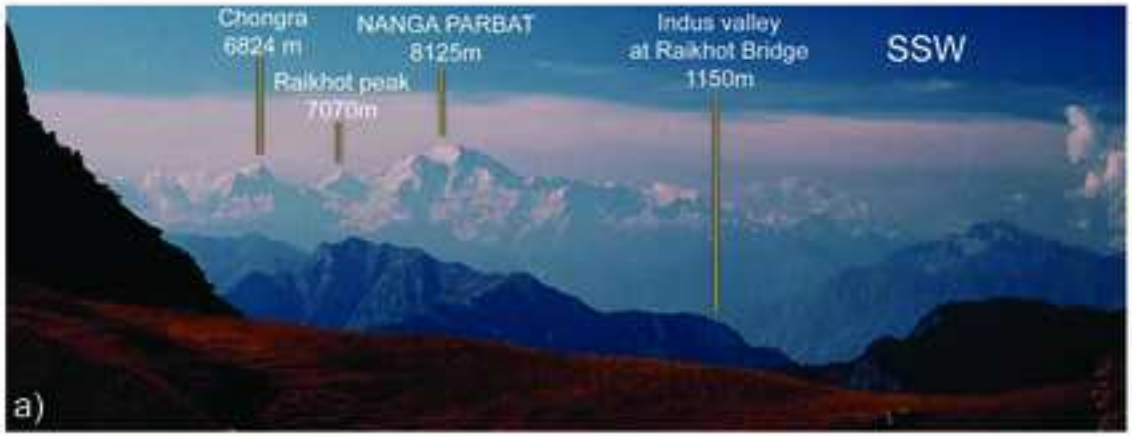

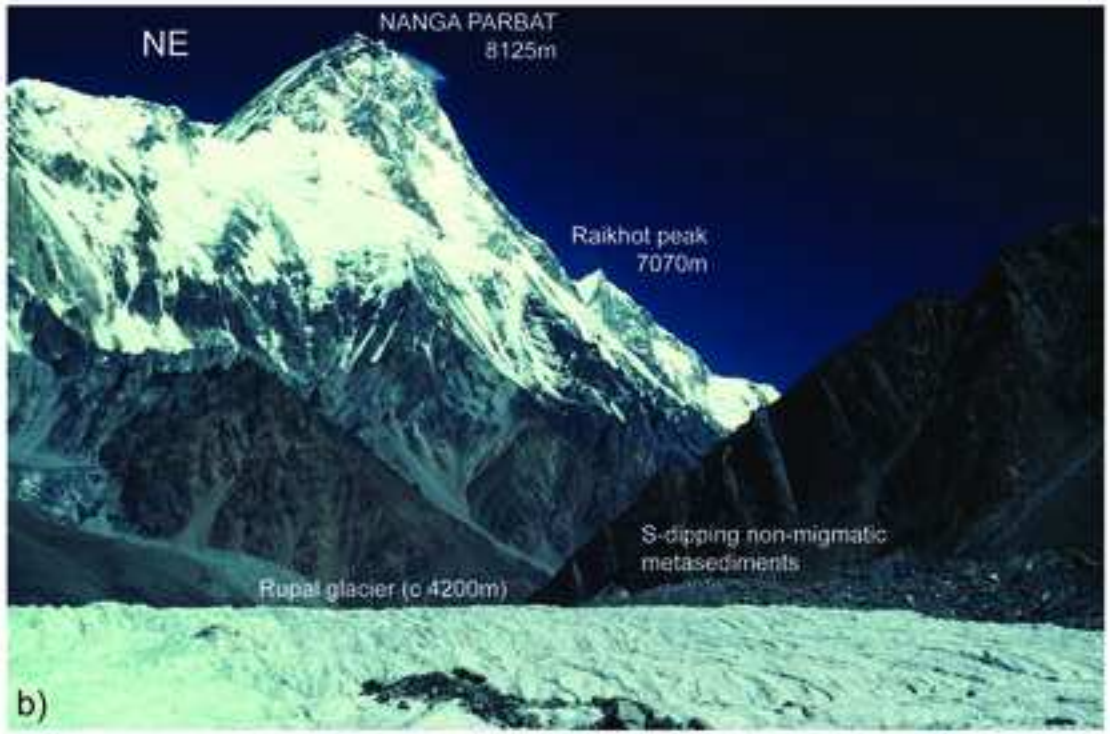

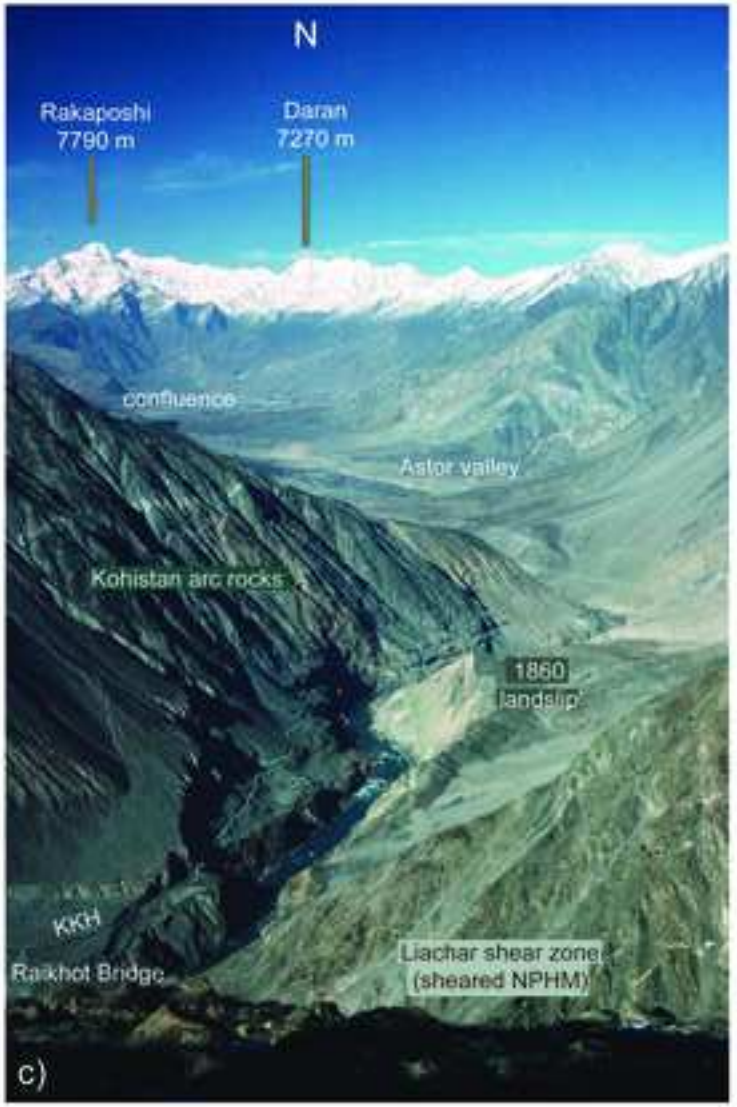

Figure 4B

Click here to download Figure Fig 4b NPHM photos b.jpg

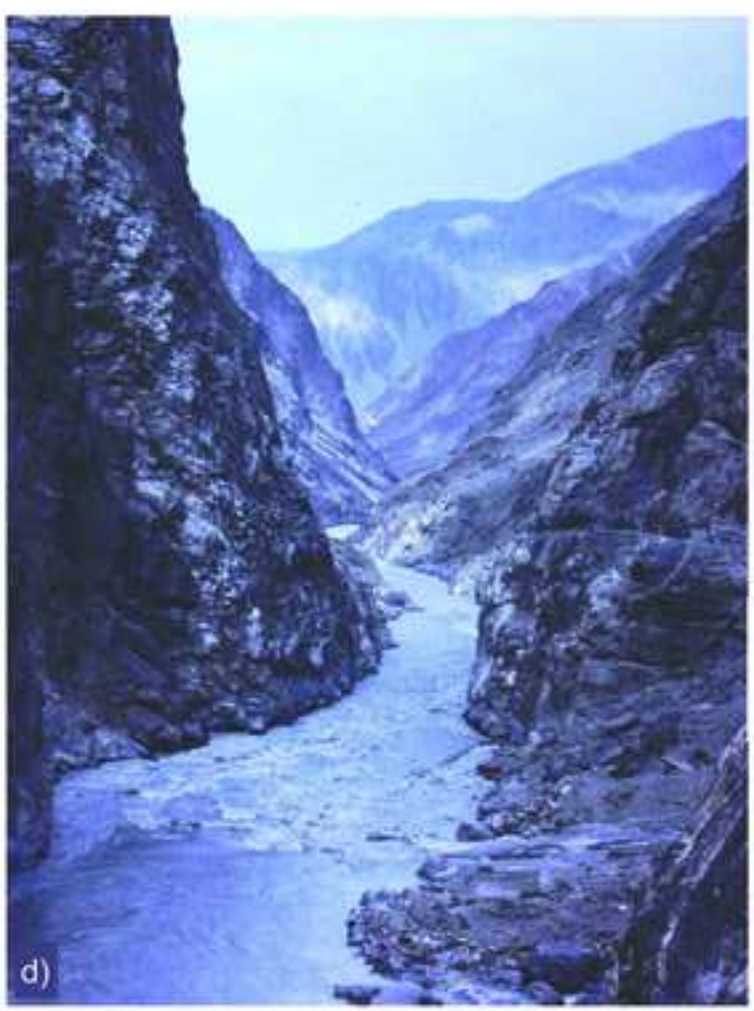

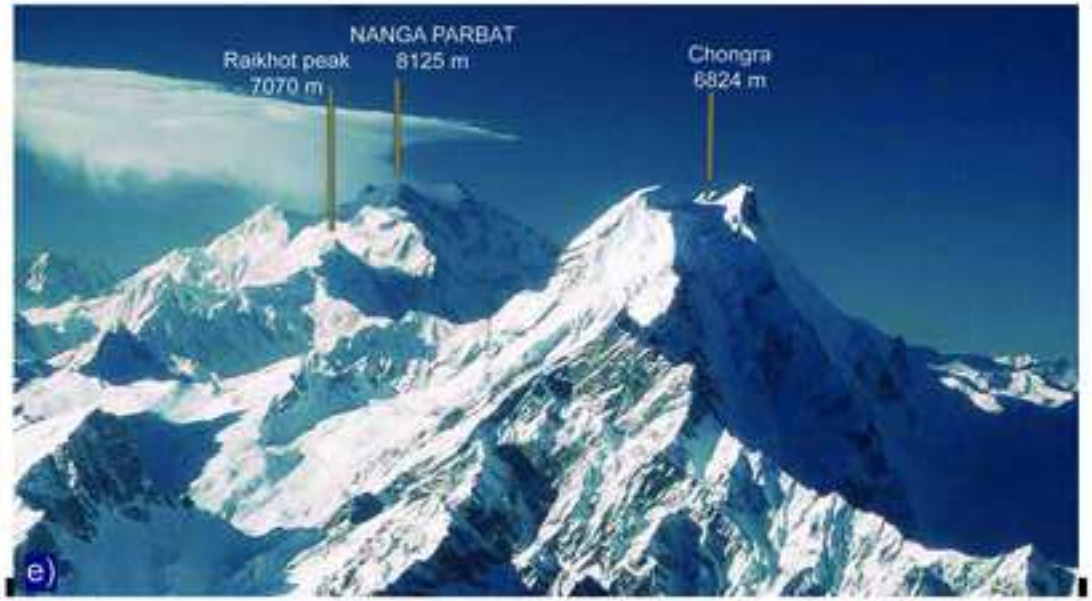

Figure 5

Click here to download Figure Fig 5 basement rocks.jpg

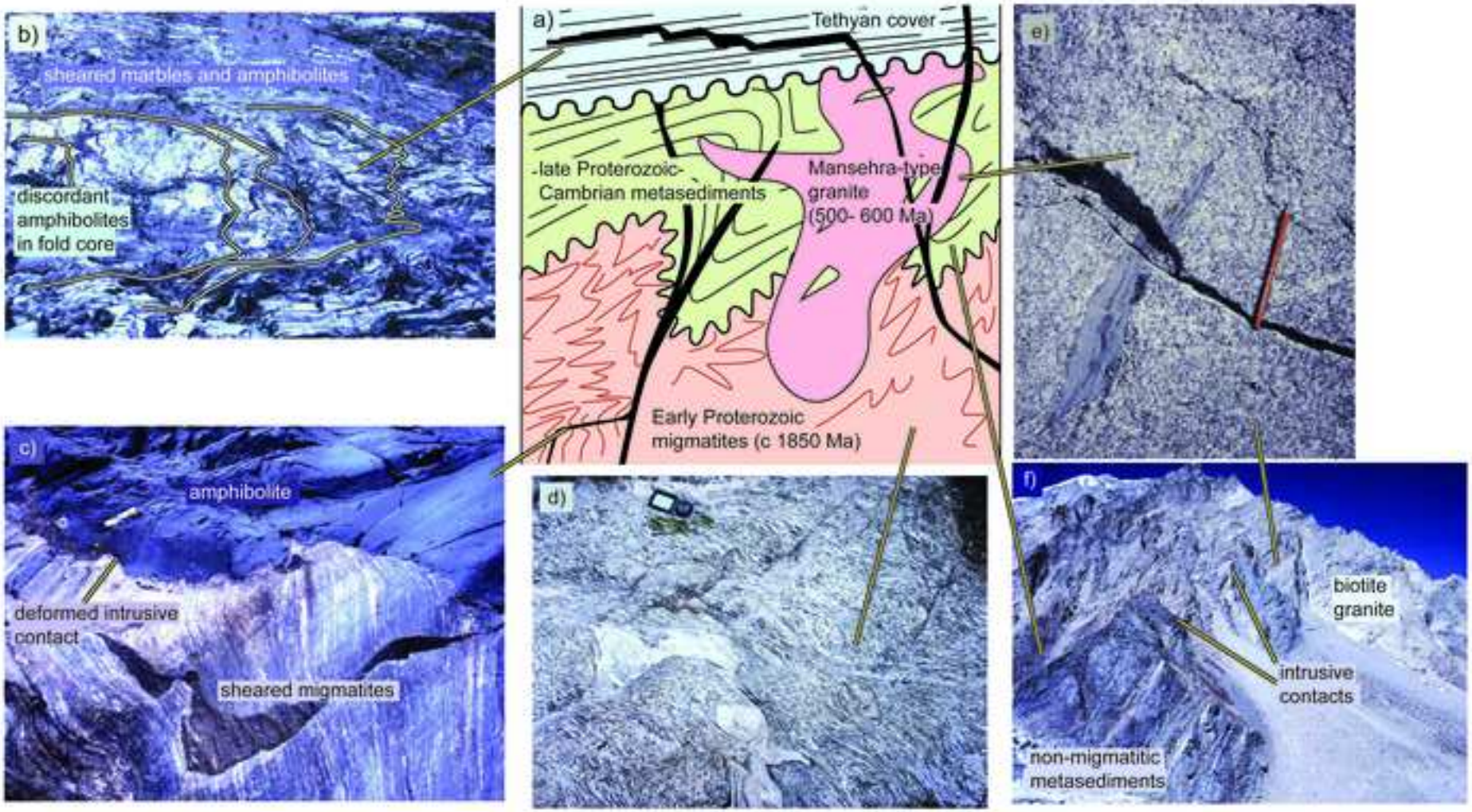

Figure 6A

Click here to download Figure Fig 6a PhuparashStak.jpg

Figure 6B

Click here to download Figure Fig 6b Sassi outcrops.jpg

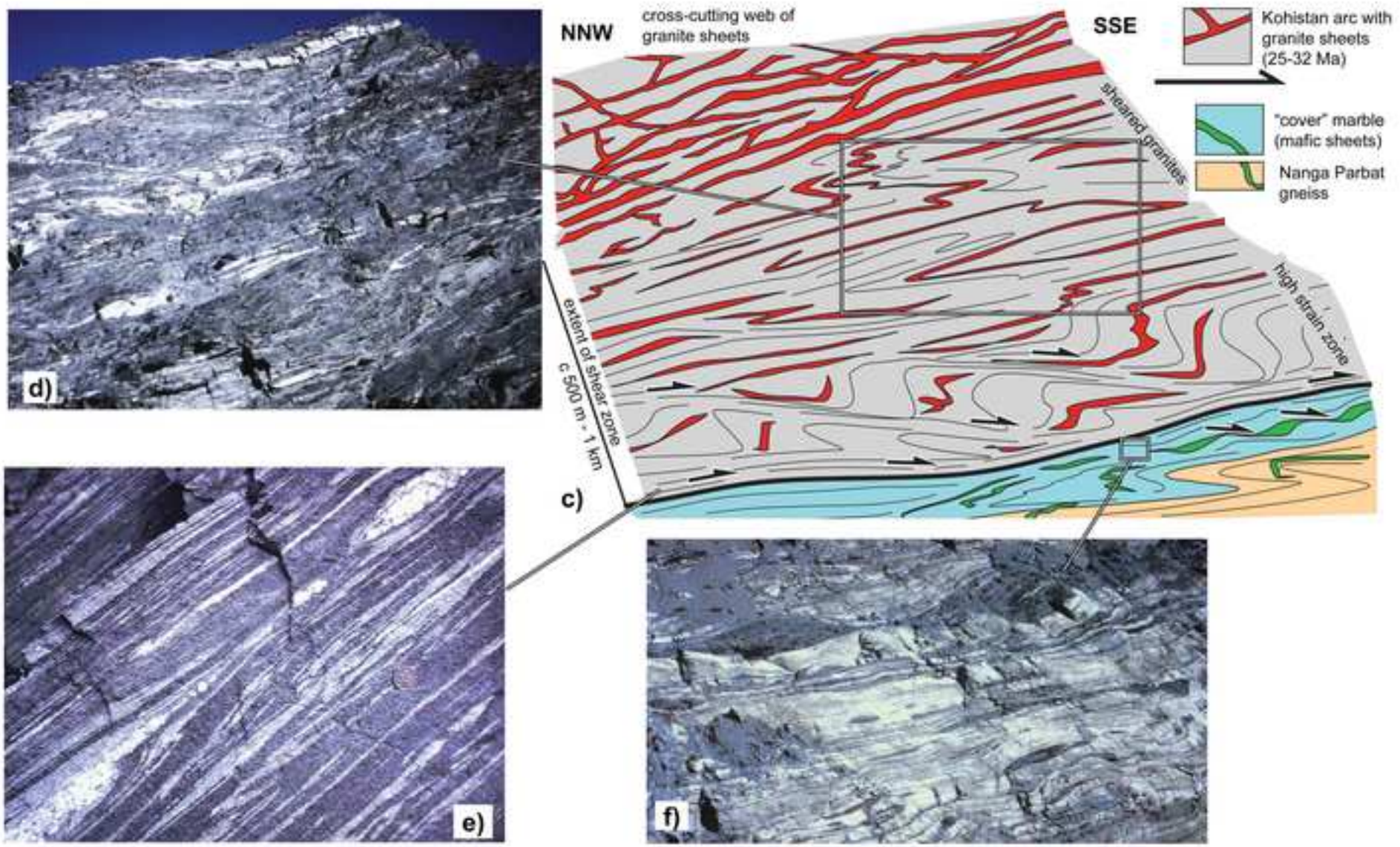

Figure 7

Click here to download Figure Fig 7 NP_PT.pdf

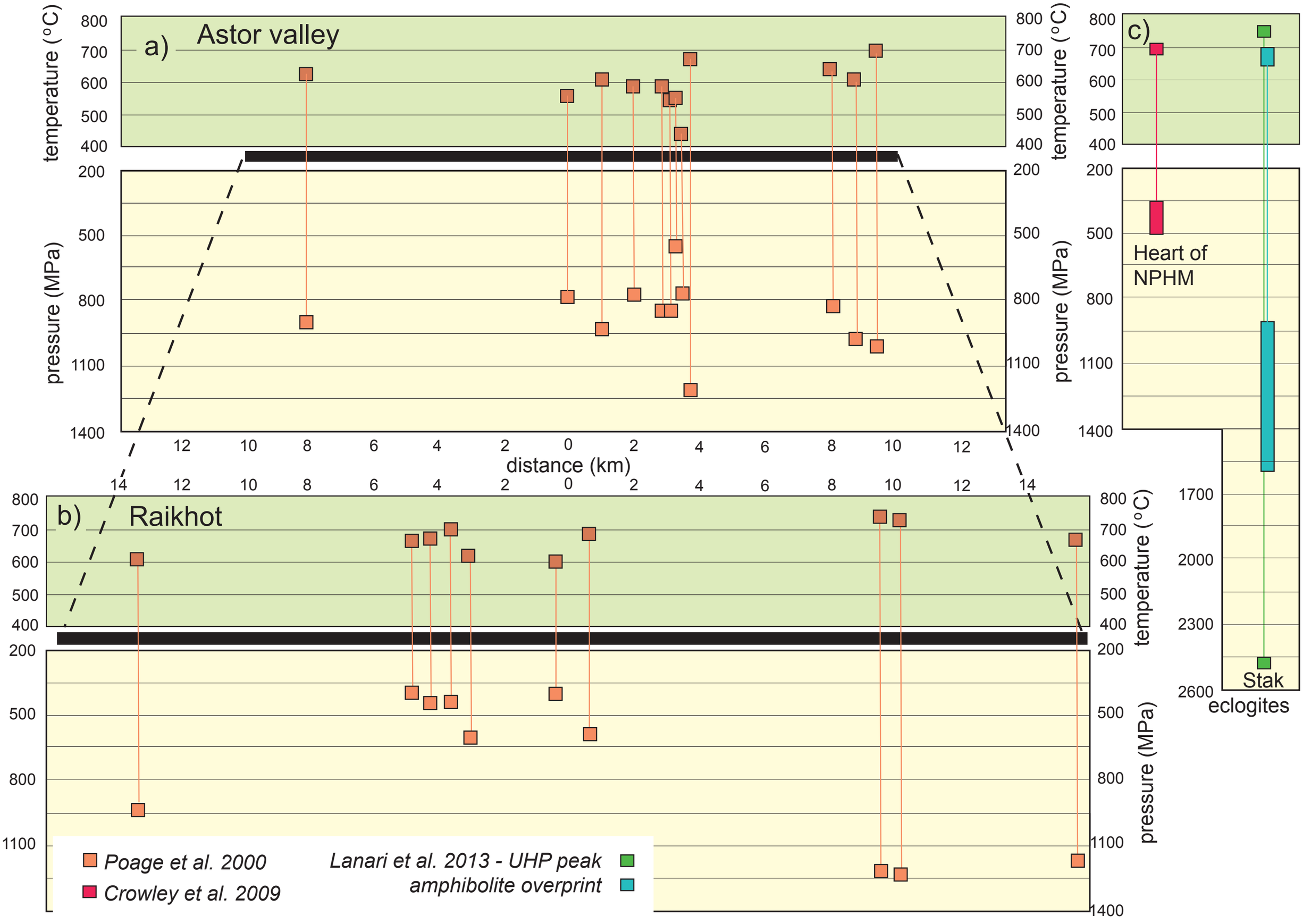

Figure 8

Click here to download Figure Fig 8 crustal models.pdf

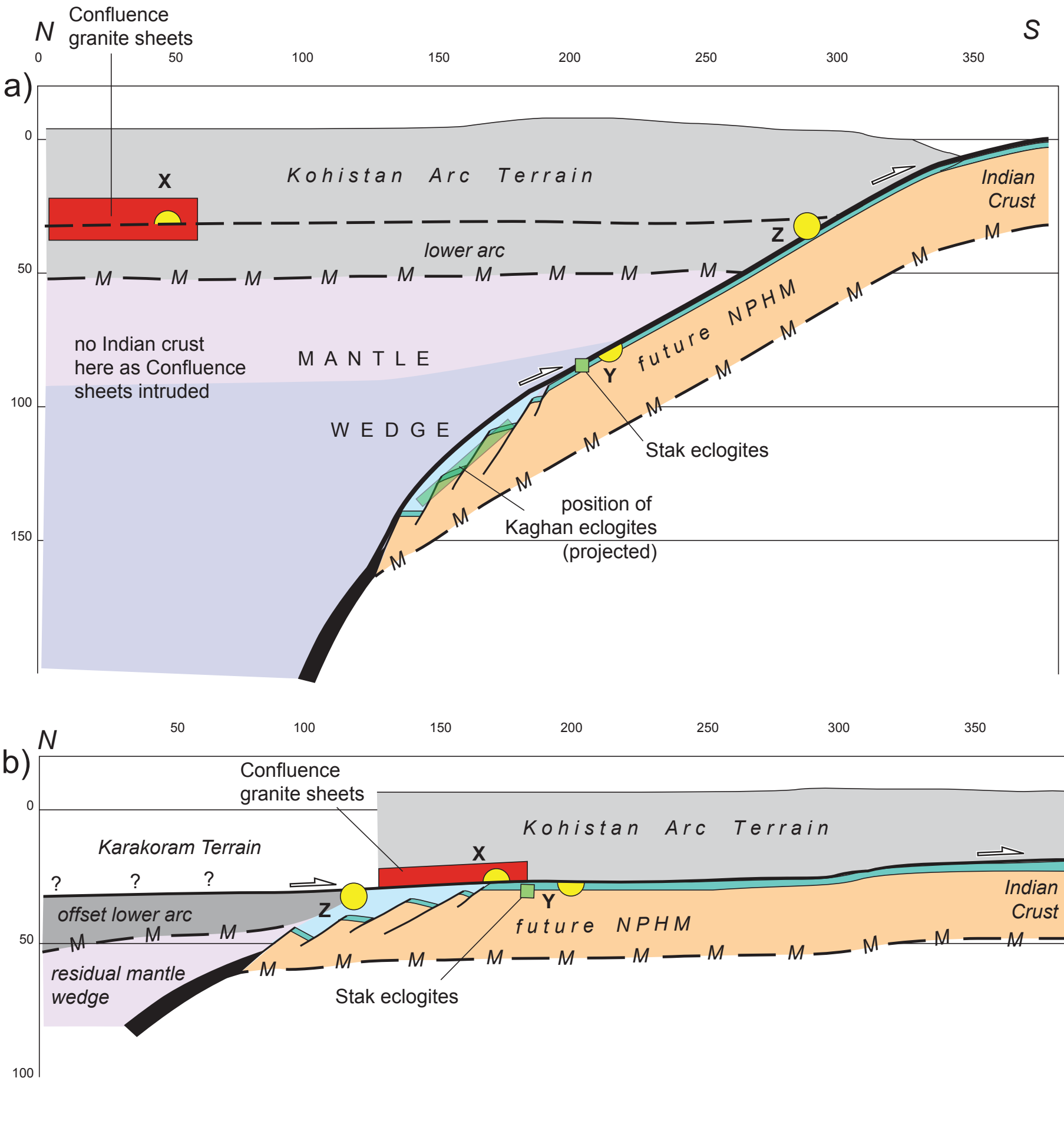

Figure 9

Click here to download Figure Fig 9 NPsections.pdf

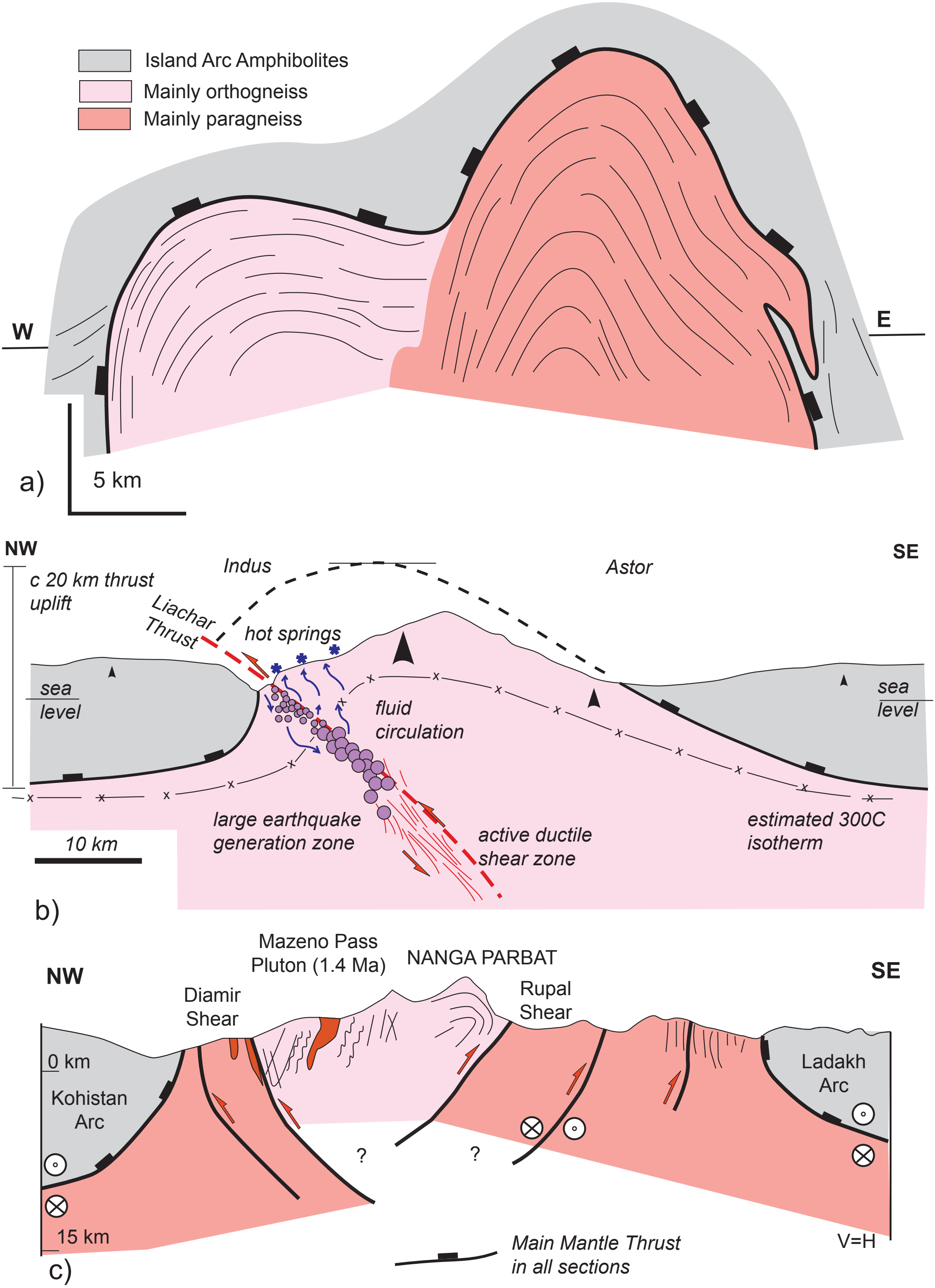

Figure 10A

Click here to download Figure Fig 10a granite shots.jpg

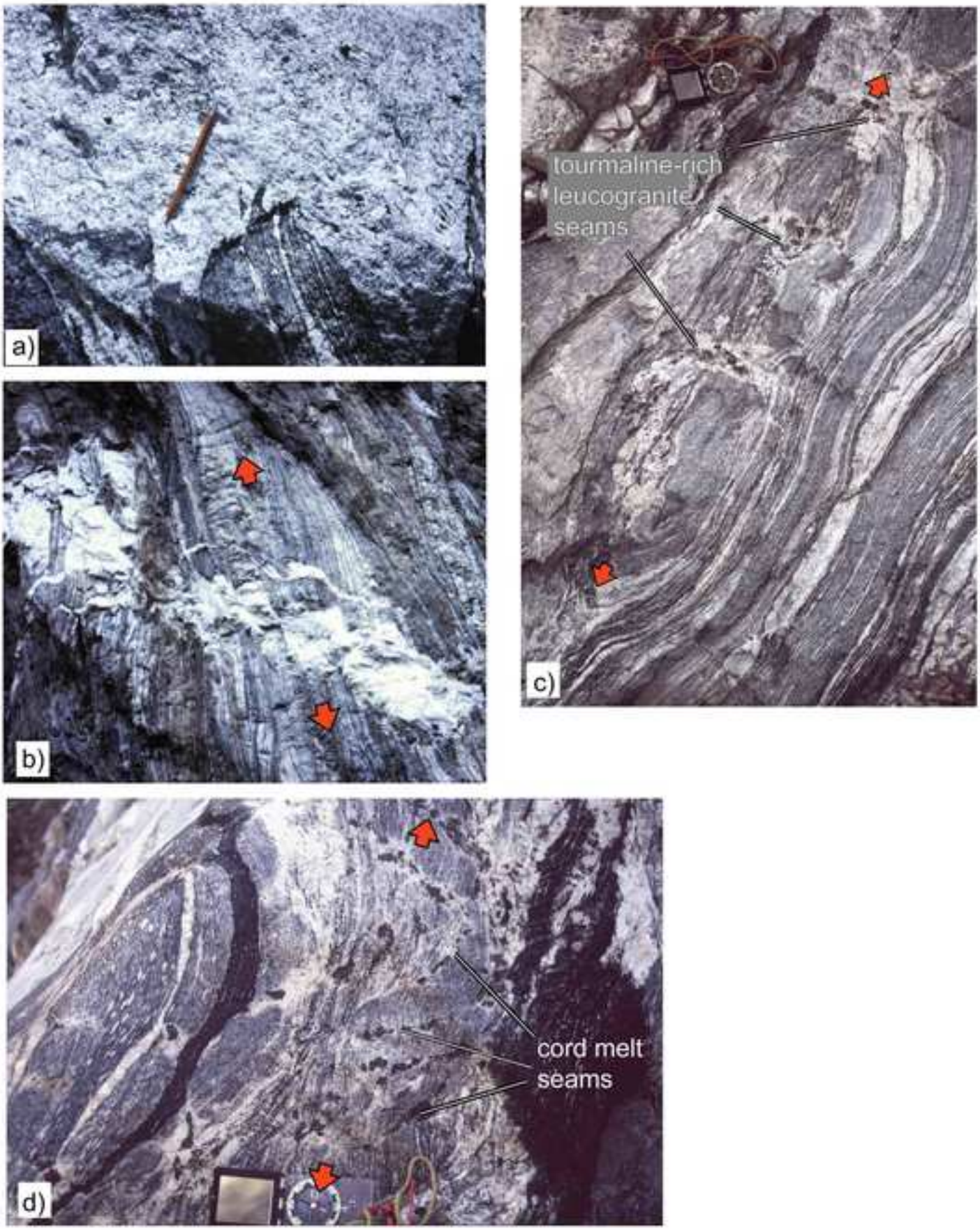

Figure 10B

Click here to download Figure Fig 10b granite shots .jpg

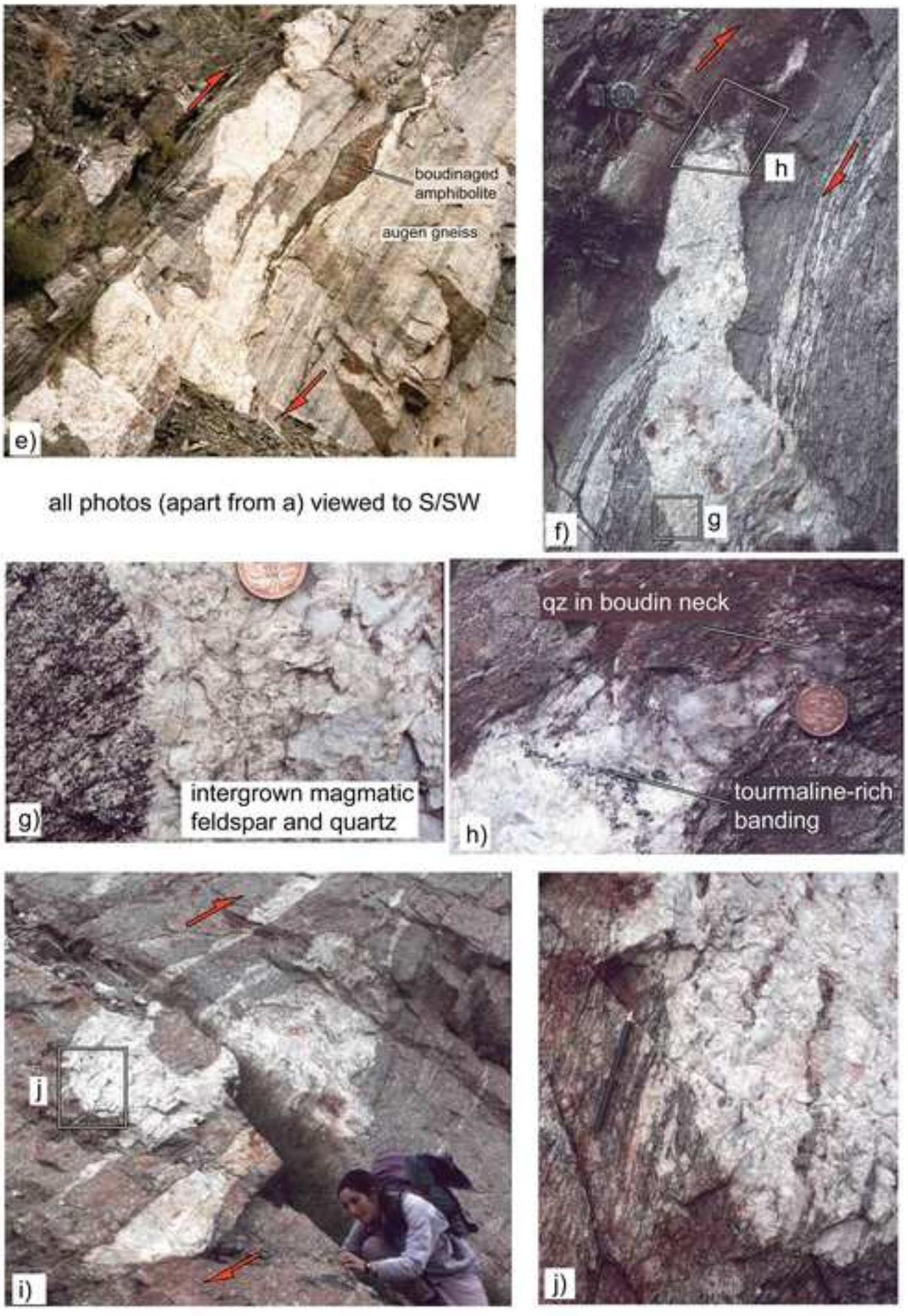

Figure 11

Click here to download Figure Fig 11 FT data.pdf

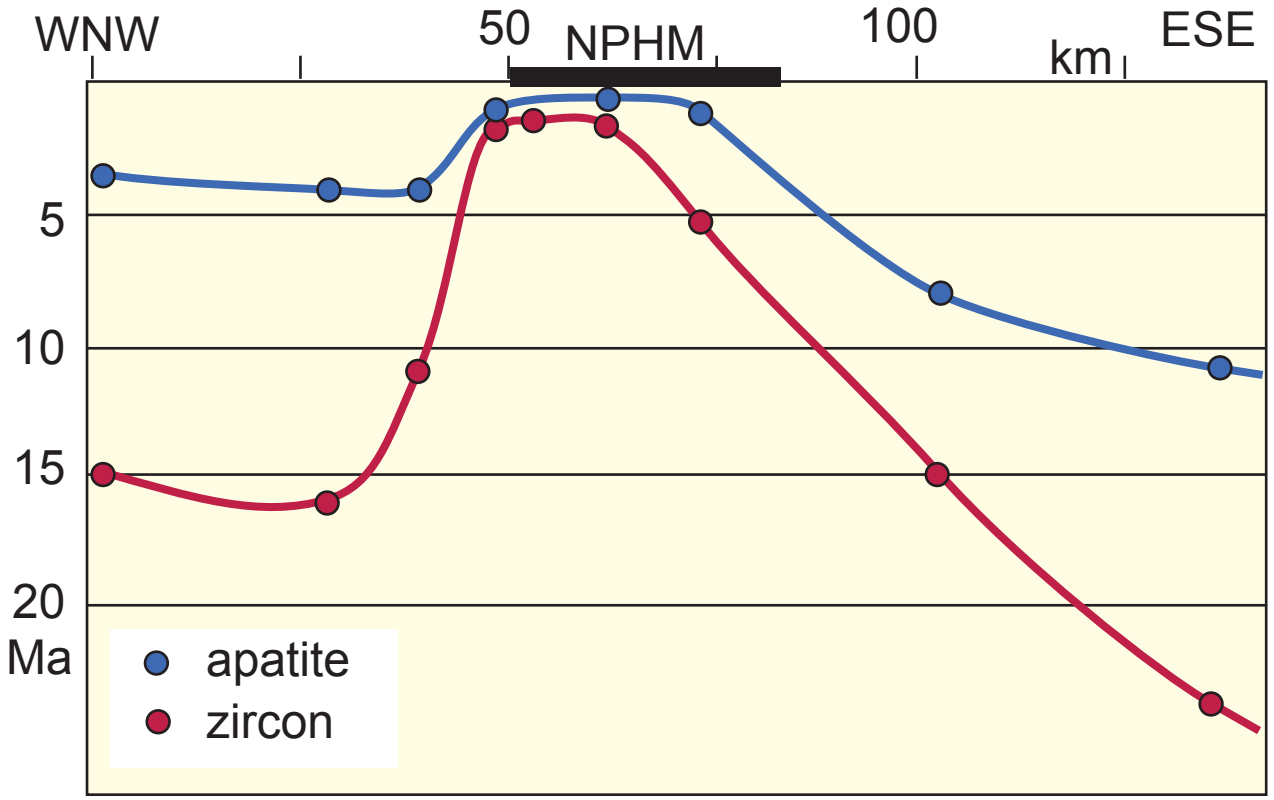

Figure 12

Click here to download Figure Fig 12 Raikhot section plus.jpg

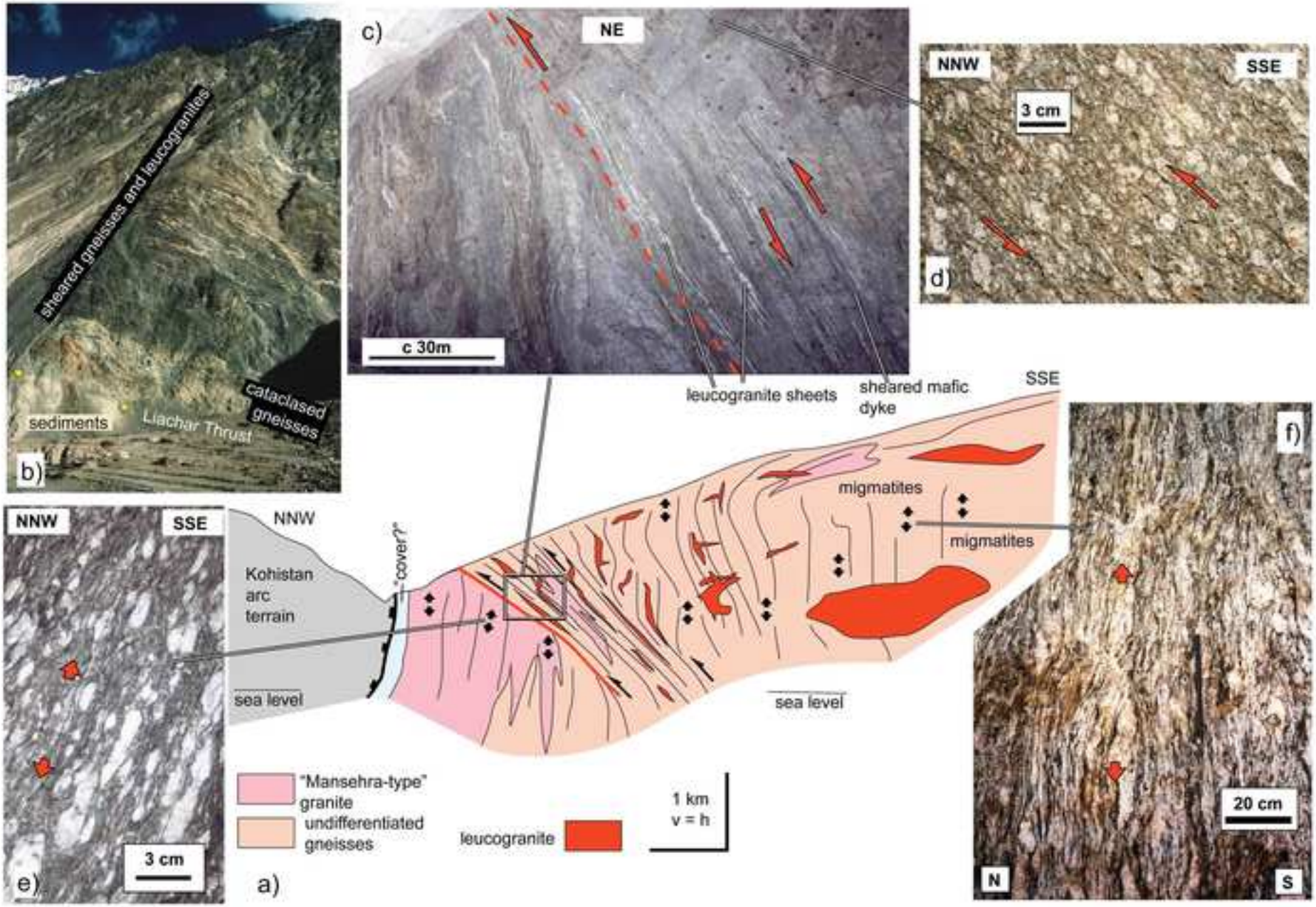

Figure 13

Click here to download Figure Fig 13 newNPsection.pdf

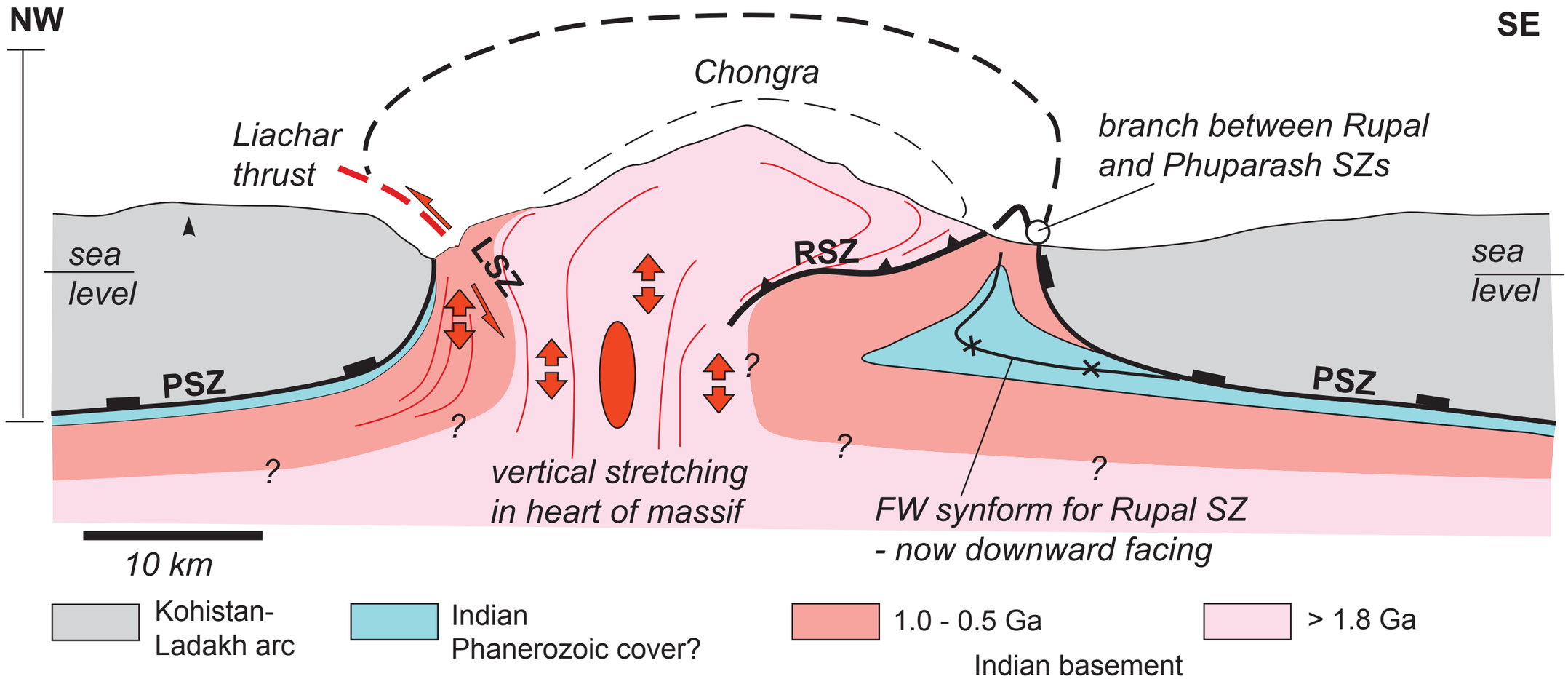

Figure 14

Click here to download Figure Fig 14 PT strength.pdf

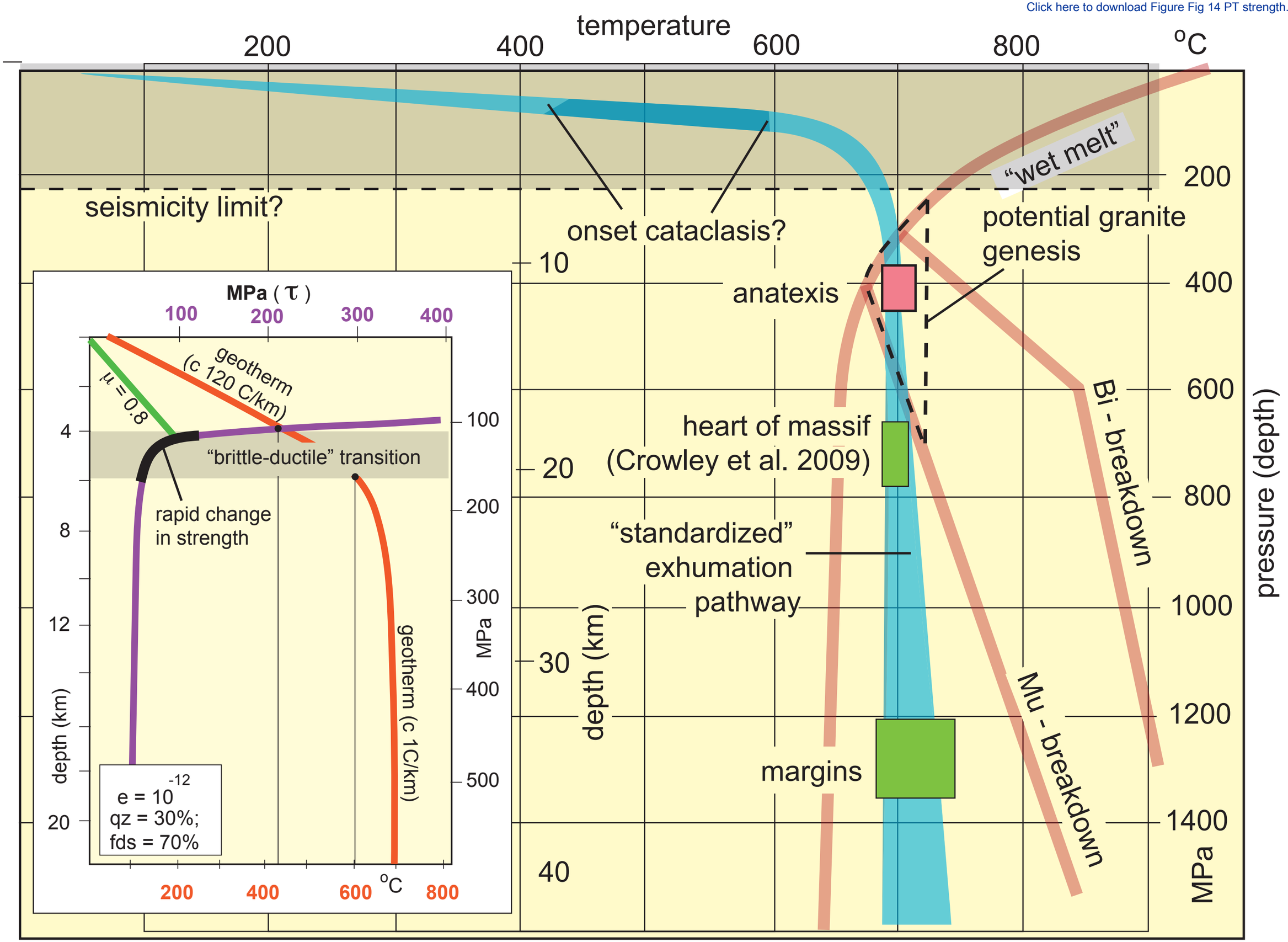

Figure 15

Click here to download Figure Fig 15 finalNamche Barwar geol map.pdf

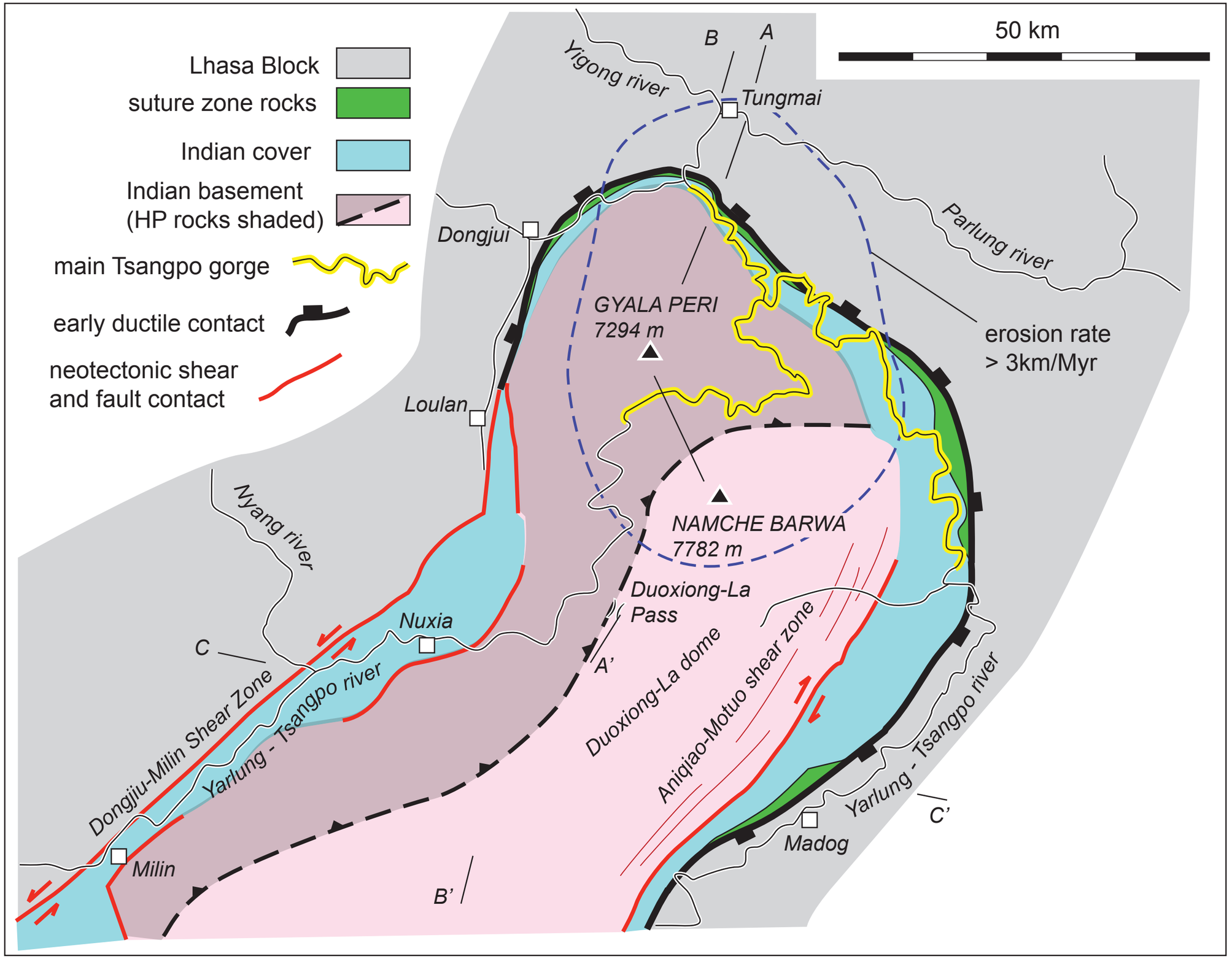

Figure 16

Click here to download Figure Fig 16 NB sections.pdf

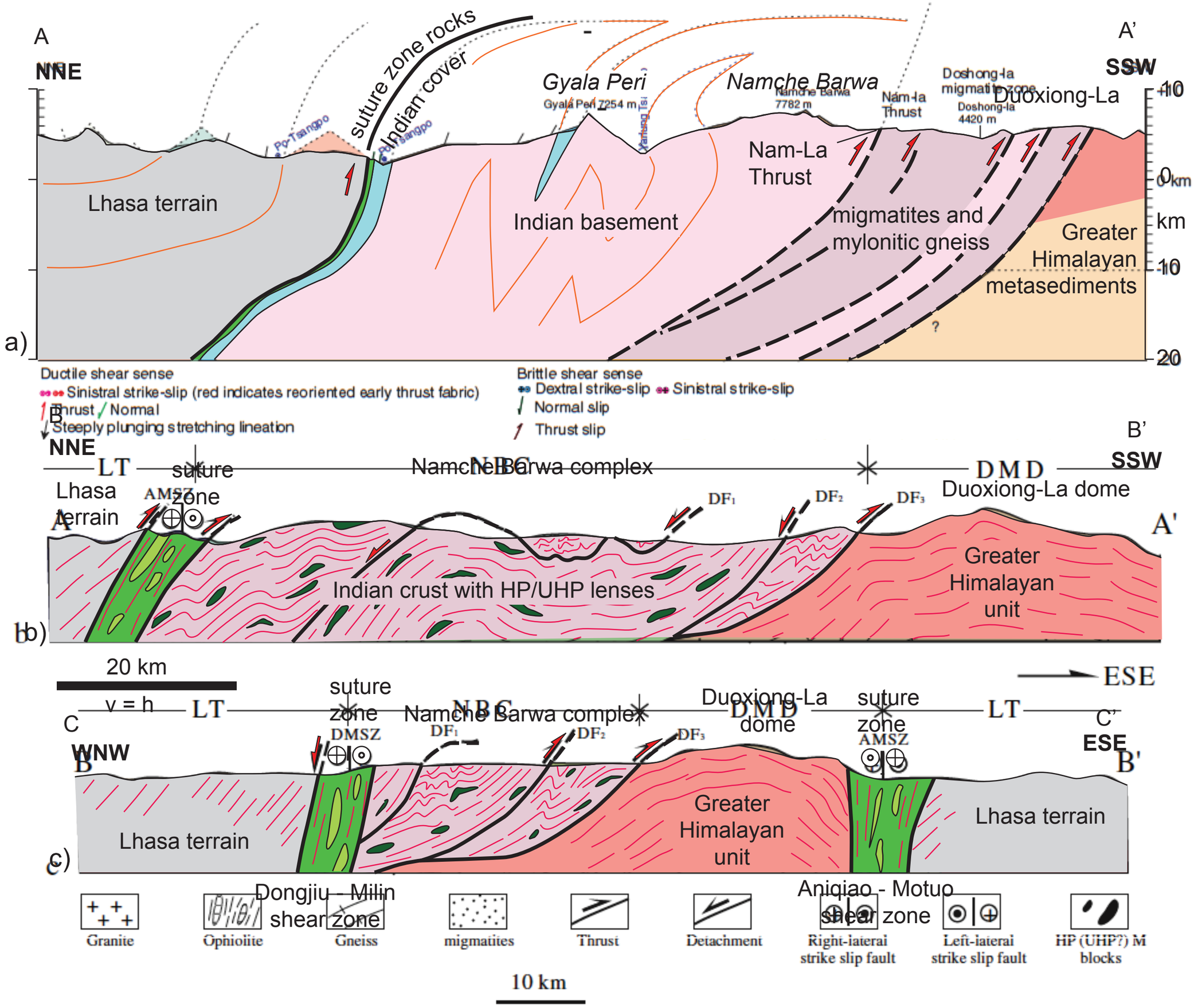

metamorphic evolution of the eastern Himalayan syntaxis

Figure 17

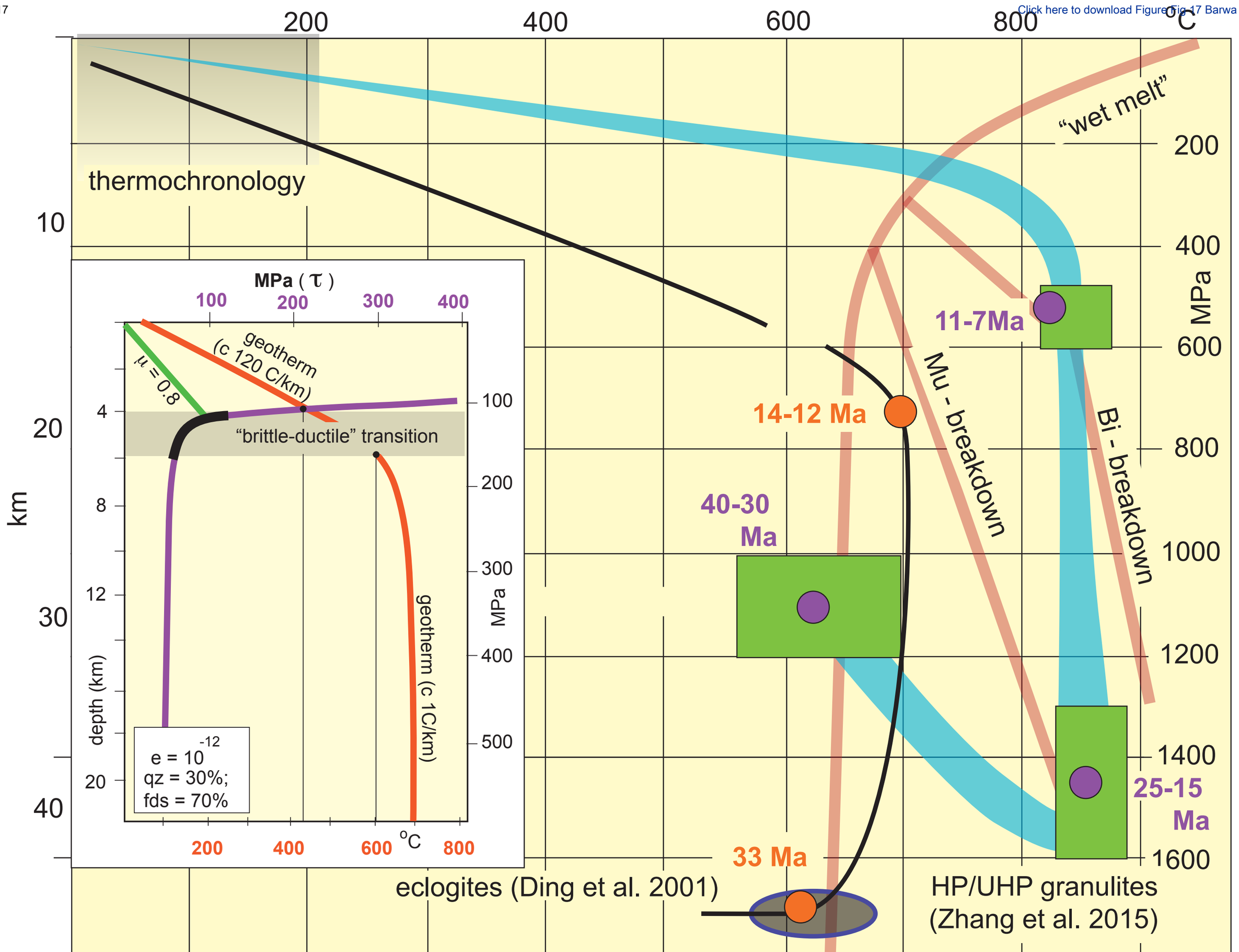

Figure 18

Click here to download Figure Fig 18 Hazara.pdf

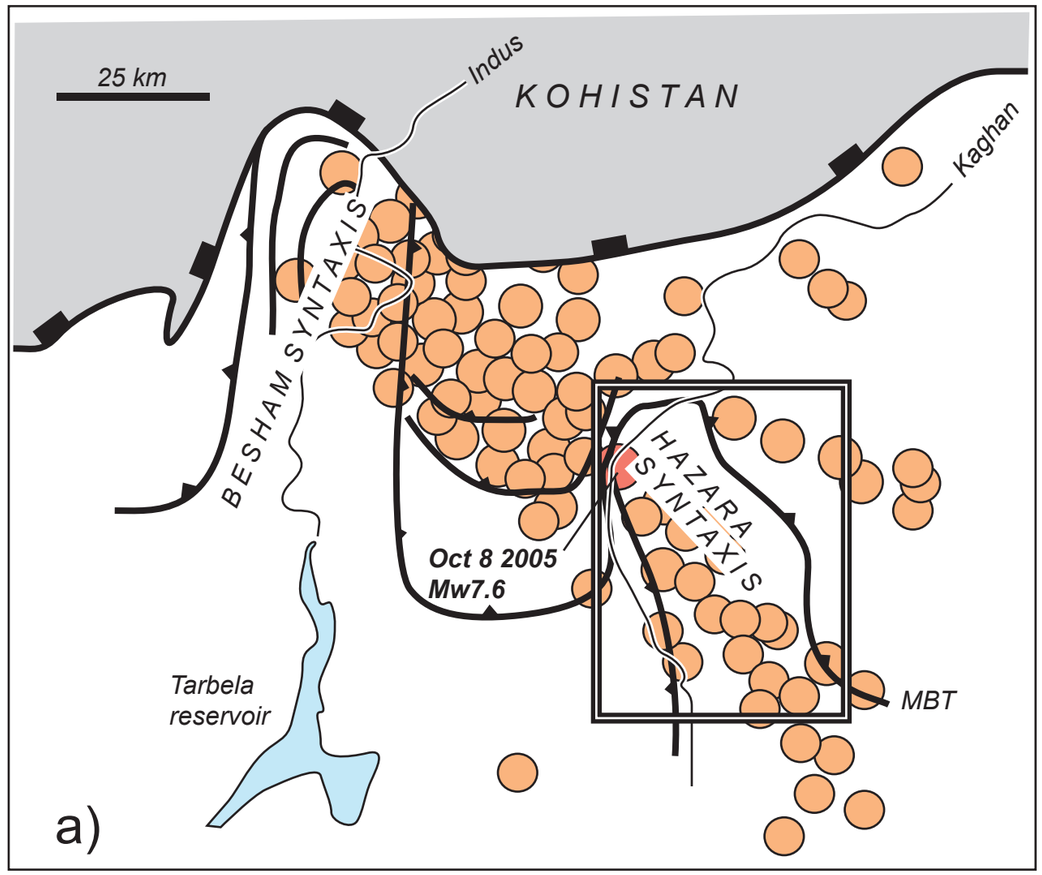

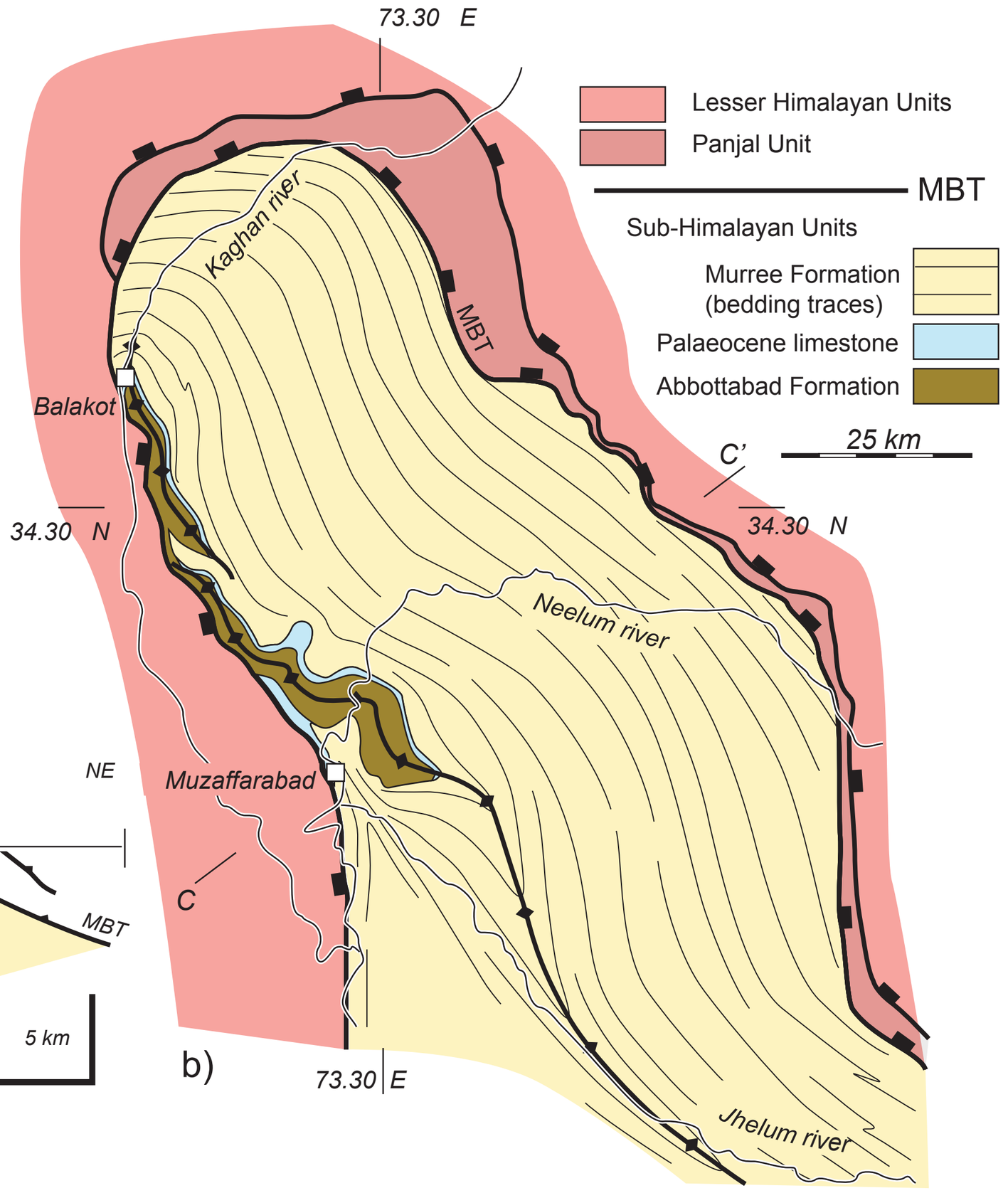

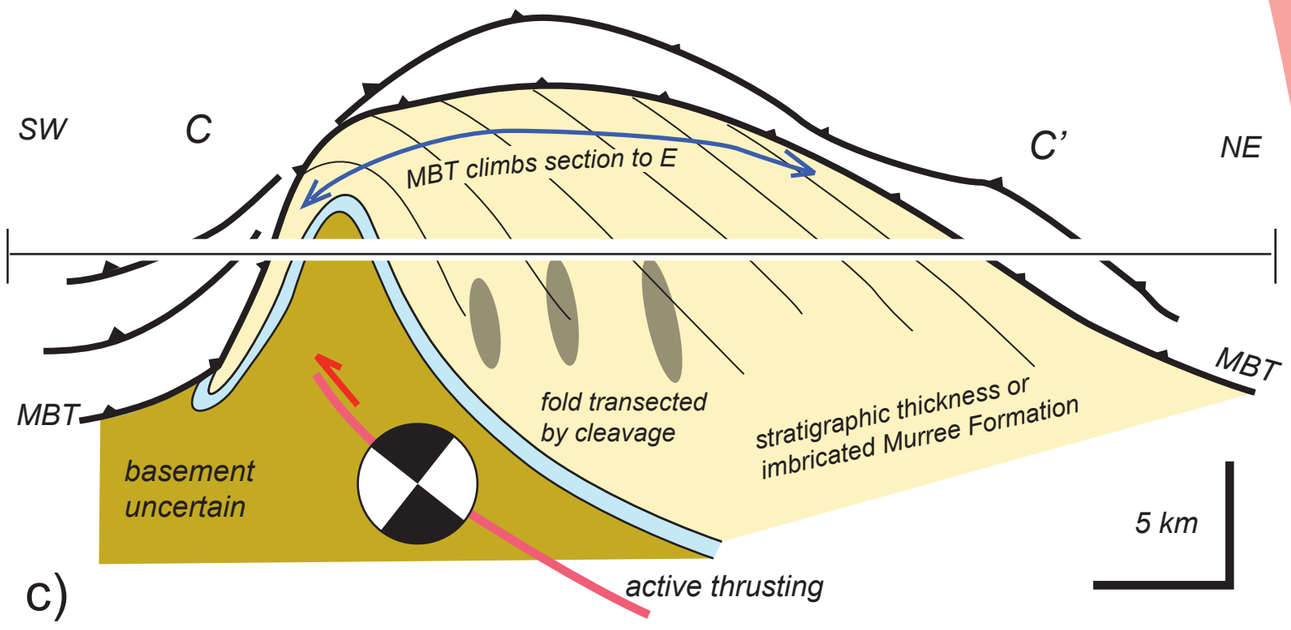

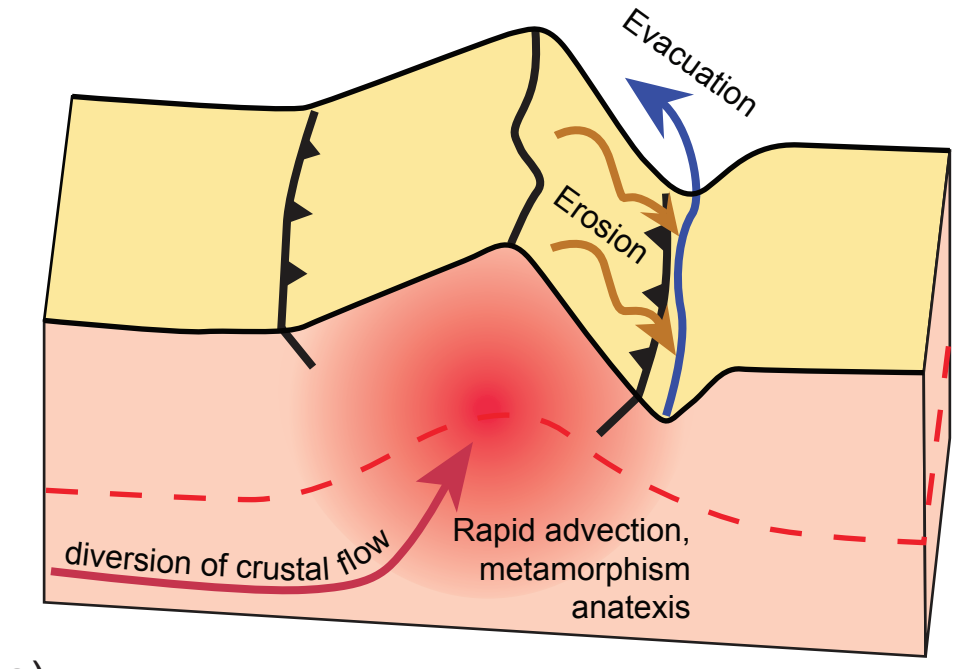

a)

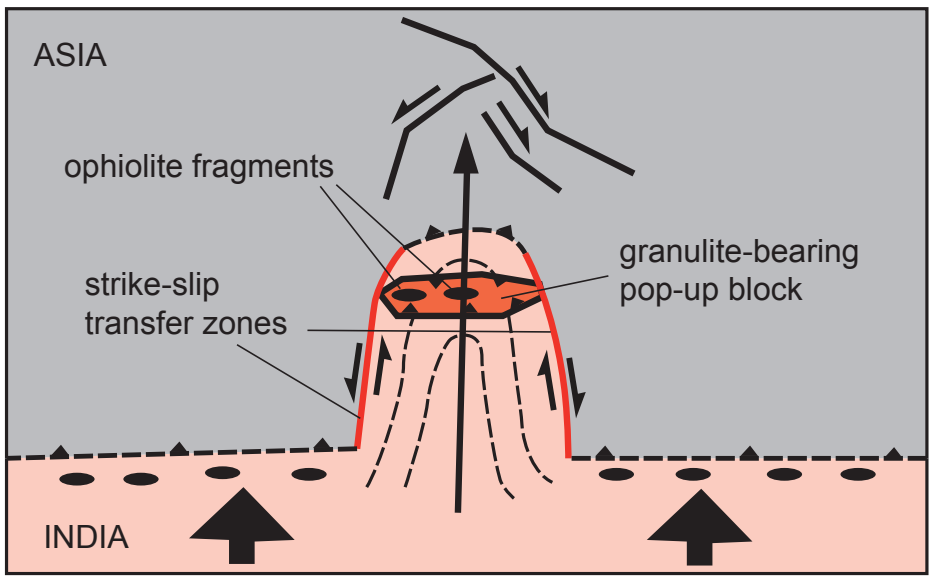

e)

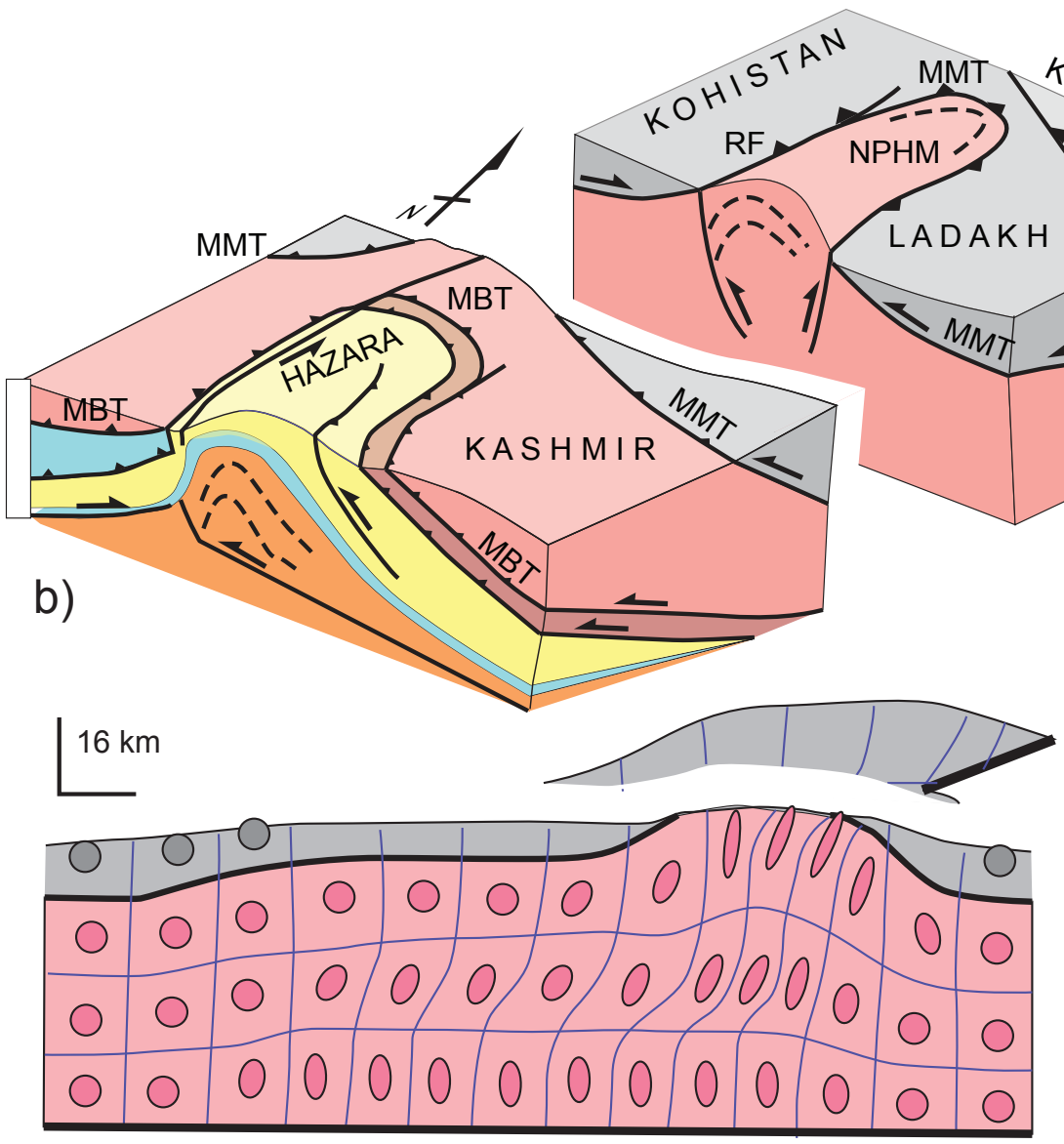

b)

c)

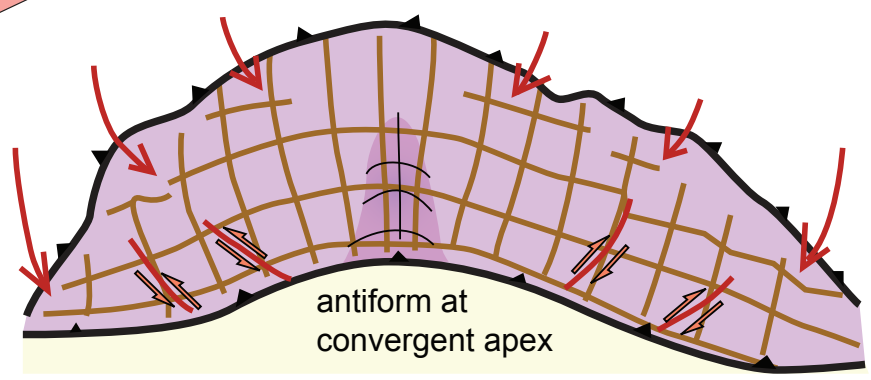

f)

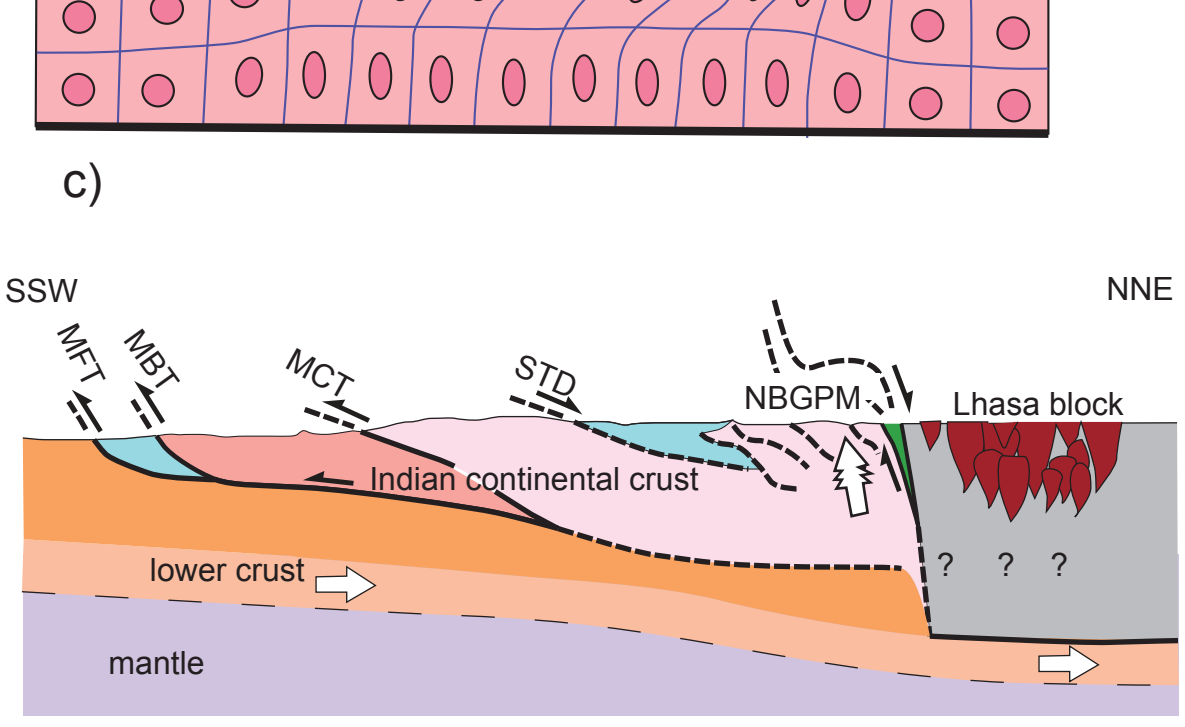

d)

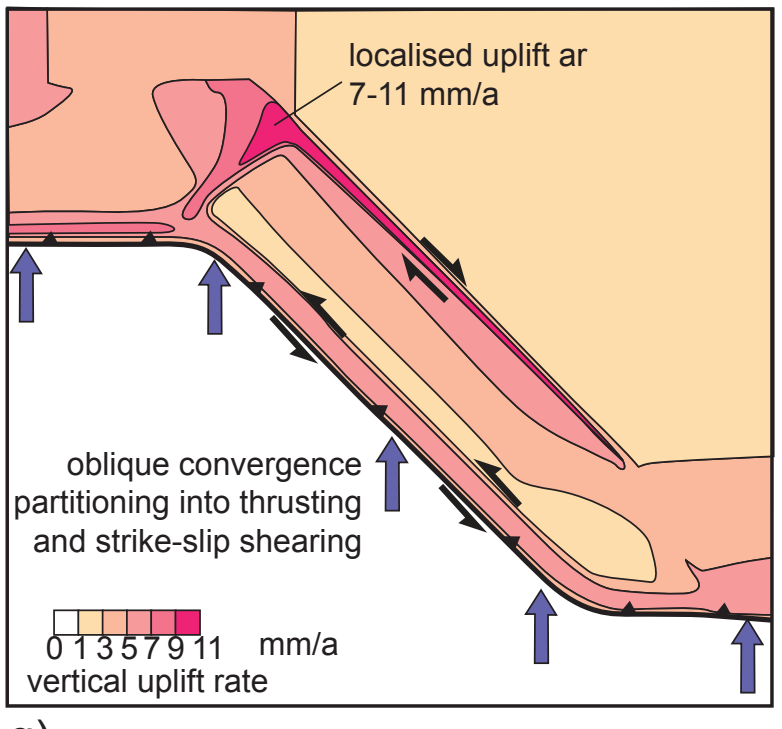

g)

Figure 20

Click here to download Figure Fig 20 Himalayan model.pdf